

UC Irvine

UC Irvine Electronic Theses and Dissertations

Title

An investigation of microfluidic produced hydrogel vesicles for artificial antigen-presenting cell applications

Permalink

<https://escholarship.org/uc/item/0834x8m0>

Author

Chen, Lindsay

Publication Date

2021

Peer reviewed|Thesis/dissertation

UNIVERSITY OF CALIFORNIA,
IRVINE

An investigation of microfluidic produced hydrogel vesicles for
artificial antigen-presenting cell applications

THESIS

submitted in partial satisfaction of the requirements

for the degree of

MASTER OF SCIENCE

In Biomedical Engineering

by

Lindsay Chen

Thesis Committee:

Professor Abraham Lee, Chair

Assistant Clinical Professor Anshu Agrawal

Associate Professor Michelle Digman

Table of Contents

List of figures	2
List of table	3
Acknowledgements	4
Abstract of the thesis	5
Chapter 1: Introduction	6
1.1 Problem statement	6
1.2 Proposed solution	6
1.3 Scope of report	7
1.4 Summary of conclusion	7
Chapter 2: Background	8
2.1 Immune response	8
2.2 How artificial cell and stiffness affect immunotherapy	10
2.3 Droplet-based Microfluidics	11
2.4 Double emulsion droplet (DED) and artificial cell	12
Chapter 3: Research Design and Methods	13
3.1 Droplet generation device and trapping array	14
3.2 Device fabrication	15
3.3 Reagent composition	15
3.4 Experiment setup and parameters	16
Chapter 4: Results and Discussion	17
4.1 Visual detection of hydrogel DED generation	18
4.2 Hydrogel DED stability, size, and stiffness	19
Chapter 5: Conclusion	26
5.1 Discussion of results	26
5.2 Limitation of the study	27
5.3 Future directions	28
Chapter 6: References	30

List of figures

		Page
Figure 1	Overview of immune response	7
Figure 2	Microstructures for droplet generation	10
Figure 3	Cell-sized unilamellar vesicles (CUV) formation	11
Figure 4	Microfluidic droplet generation design	12
Figure 5	Microfluidic trapping array design	13
Figure 6	DED generation experiment	16
Figure 7	DED size before UV	18
Figure 8	DED size after UV	18
Figure 9	DED morphology before added into RPMI	19
Figure 10	DED morphology after added into RPMI	20
Figure 11	Non-crosslinked DED under 0 ul/min flow rate	21
Figure 12	Non-crosslinked DED under 10 ul/min flow rate	21
Figure 13	Crosslinked DED under 5 ul/min flow rate	22
Figure 14	Crosslinked DED under 10 ul/min flow rate	23
Figure 15	Potential DED measurement error	25
Figure 16	Microfluidic stiffness sorting design	27

List of tables

		Page
Table 1	Pressure pump setting for 5%, 10%, 15%, and 20% PEGDA hydrogel double emulsion droplet generation.	14
Table 2	Composition of external phase, oil phase, and internal phase, as well as overall experimental condition design.	14
Table 3	Crosslinked and non-crosslinked hydrogel DED stability.	17

ACKNOWLEDGEMENTS

I first want to thank my mentor Becky for training and helping me throughout my entire experiments, from device setting, fabrication, and all the experimental design. Without her, the project would never have been started. I also thank Evan, my lab member, for assisting me in stiffness examination, especially the trapping array designed by him, giving me a little hope for my experiment. I want to extend special thanks to Shawn and Song for giving up hours of their time to and discuss and find solutions to the difficulties I encountered. Without you, this thesis would not have been possible. I will never forgot the time we spent in lab. Another huge thank you to everyone in BioMiNT lab at UCI. Your support was incredibly encouraging.

I would like to thank all my friends, Allen and Vivian, and my family supporting me pursuing my dream and reminding me when it is time to take a break. I also appreciated my supervisor and colleague, Terry, in my company, giving me flexibility and assisting me on my work.

Lastly, I would want to express my gratitude to my thesis committee chair and advisor, Dr. Abraham P. Lee for providing me an opportunity joining into the lab and developing my career, working and studying at the same time. I am grateful for the guidance and support, especially your passion in microfluidics and innovated ideas keep me moving forward when experiments did not go as planned. I would like to thank my committee members Dr. Digman for supporting me earning my degree and Dr. Agrawal for collaborating with our project, providing cell samples and kit. Without you, this project would not be completed.

ABSTRACT OF THE THESIS

An investigation of microfluidic produced hydrogel vesicles for artificial antigen-presenting cell applications

By

Lindsay Chen

Master of Science in Biomedical Engineering

University of California, Irvine, 2021

Professor Abraham P. Lee, Chair

The antigen-presenting cell is the key component in T cell activation pathway, delivering signals and helping T cell detecting and fighting cancers. Research have reported that T cells are mechano-sensitive to the environment. Their activation, differentiation, recognition, and function are regulated by mechanical forces such as contact tension, shear stress, and substrate rigidity. However, the examination on how the stiffness of artificial antigen-presenting cells (aAPCs) affects T cell's functions remains unknown. Therefore, in this research, a novel microfluidic-based double emulsion droplet (DED) generation chip is proposed to generate monodisperse hydrogel DEDs with tunable stiffness and fluid membrane. Another trapping array device is used to exam the stiffness differences between crosslinked and non-crosslinked Polyethylene (glycol) Diacrylate (PEGDA) hydrogel DEDs. The result shows the hydrogel DEDs have a significant difference in stiffness before and after the UV exposure. The hydrogel DED's stability decreased as the hydrogel concentration increased. Also, we discovered that the trapping array can be a potential candidate for DED dewetting, as it shortens the dewetting process to less than 20 seconds.

Chapter 1: Introduction

1.1 Problem statement

According to the statistic, cancer is the second of the leading causes of death in United States⁶. After spending millions of dollars on cancer research, scientists still cannot find a general treatment to this disease since each cancer has a different response to treatments⁷. Treating cancer becomes more difficult since cancer cells can target T cells and deactivate them, allowing cancer cells hidden from immune response^{12,17}. Cancer cells can also mimic healthy cells, trick the body to form blood vessels, which is called angiogenesis, and help them get the oxygen and nutrients¹¹. Moreover, sometimes the new drugs work on the lab-growing cells may be failed when doing the clinical trials on patients¹³. Traditionally, we have treated cancer by attacking it with chemotherapy and radiation, or by removing it with surgery⁸. Nonetheless, there are some side effects: surgery could cause the damage to other organs or tissues, hair follicles cells could be damaged by chemotherapy, and some patients may experience the skin dryness, itching, or peeling¹⁴. All these information indicate that either getting improvement based on current treatments or finding novel methods to cure cancer is needed.

Nowadays, some researchers have synthesized mesoporous silica microrods coated with liposomes to assemble antigen-presenting cell (APC) -mimetic scaffolds, and the results showed that the number of T cell expansion can support clinical level T cell manufacturing (starting with 10^5 to over 10^9)¹⁰. Others also validated that T cell could sense the mechanical force from the environment and more numbers of T cell will be activated in a stiffer substrate¹⁵. However, there are limited research regarding the method of changing the stiffness of artificial antigen-presenting cells (aAPC). Additionally, since traditional artificial cells are hard to be tuned for their stiffness, most of the research only demonstrated that T cell activation level depends on the environment stiffness, lacking of the result about the relation between T cells and the stiffness of the APC they interact with, especially the cytotoxic T cell activation pathway which is triggered from APC. Therefore, it is important to have a novel method to fabricate aAPC with tunable stiffness and fluid membrane, which affects the diffusion of proteins within the membrane.

1.2 Proposed solution

The mechanism behind the immune system fighting against cancer is important since we can boost our body's natural immune response and help it detect and kill tumor and cancer cells in a more effective and efficient way. Several different types of immunotherapies that are used to treat cancers have been well published, and we can divide them into active and passive according to the stimulation of the host system²⁶: active immunotherapy boosts and triggers host defences; while passive immunotherapy transfers tumor-targeting monoclonal antibodies or molecules to patients. Cell-based immunotherapies, which include ex vivo transfer of tumor-infiltrating lymphocytes, engineered T cells, and in vivo checkpoint inhibitors to stimulate lymphocytes, are also known as adoptive cell transfer; and such therapy can be passive - helping and using our own immune cells to eliminate cancer cells²⁵. Cancer vaccines trigger anti-tumor response in our immune system to recognize cancer and since dendritic cell is the most effective APC and play an important role in immunologic memory establishment, it is widely selected for tumor vaccines^{12,27}. Among all, cell-based immunotherapy attracts more attentions since more and more studies suggest that APC – particularly dendritic cell – play a pivotal role in recognizing tumor specific antigen, initiating the adaptive immune response⁵. Using aAPC as anti-cancer response then transfer the activated T cells back to patients can deal

with problems caused by autologous APC such as time-consuming and costly²⁹. Furthermore, T cell signaling would be easier to control.

Producing artificial cells by microfluidics has been developed over the years and have overcome problems associated with conventional methods such as sized monodispersity⁴. Using flow focusing as the geometry to form double emulsion droplets formation benefits the lipid bilayer study since it has the potential to produce thinner middle oil layers; therefore, mimicking natural immune synapse on such synthetic surface more closely²⁴. The other advantage would be its high throughput and high encapsulation efficiency.

Previous research validated that T cell is a mechano-sensor and some studies have already shown that higher activation marker is expressed, and proliferation increases when T cells contact on stiff substrates¹⁵. But activating T cell with cell-sized hydrogel beads as artificial APC has not be reported yet. Here we propose by using microfluidics to generate hydrogel DEDs. We successfully encapsulated different concentrations of Polyethylene (glycol) Diacrylate (PEGDA) into oil phase, and possibly tuned the stiffness of the microgel, which not only mimics the fluid nature of cell membrane but also maintains their size uniformity, in order to increase the effectiveness over other approaches towards aAPCs.

1.3 Scope of report

This thesis aims to provide the purpose, design, methods, results, and the outlook on stiffness tuning PEGDA hydrogel DED as the first step in generating aAPCs with fluidity membrane by microfluidics, as well as the cell stiffness validation by trapping array and microfluidics device fabrication. This report also covers an overview background on relevant immunotherapy research, artificial cell, microfluidics, and quantitative technique which are used in this study. The stability of different concentration of hydrogel droplets was calculated by hemocytometry slide and imaged the samples over one month. Stiffness comparison was examined by trapping array. The report concludes with the discussion of the result, limitation of the study, as well as future work.

1.4 Summary of conclusion

The results of this study showed that microfluidics is a promising method for hydrogel double emulsion droplet generation. By optimizing the fabrication of PEGDA hydrogel DED generated by microfluidics, which mimic the aAPC, and further investigate the relationship between their stiffnesses and T cell activation level, could be a possible solution to deal with the difficulties people encounter. In our experiments the DED stability decreased as the hydrogel concentration increased. As the result, we were able to distinguish the stiffness differences between crosslinked and non-crosslinked DEDs, which suggested that UV treatment is capable to initial crosslink reactions under the micro-scale. Unexpectedly, our results also reported the tapping array as a potential tool to extract excessive oil phase, forming cell-size unilamellar vesicles (CUVs) to better mimic aAPC. We also provided some solutions to the unexpected problems we encountered such as droplet toxicity and isolation, looking to repeat experiment several times to get a more precise result.

Chapter 2: background

2.1 Immune response

Immune system is a complex network of cells and organs which can help the body defense bacteria, virus, and other diseases. Innate immunity is the first line immune response which immediately defenses nonspecific foreign pathogens; while adaptive immunity is a long term, antigen-specific defense mechanism²¹. Lymphocytes, which are also known as white blood cells, are human body's main types of immune cells which are made in bone marrow from hematopoietic stem cells. There are two subtypes of lymphocyte: B cell and T cell. Bone marrow is the place where B lymphocytes mature, while T lymphocytes travel to thymus gland for their further development, and later receive their immunological education before they go into bloodstream²¹. The naïve T cell, which with both CD4 and CD8 markers on its surface, will first go through positive selection at thymic cortex, and only the one that has strong interaction with antigens expressed by major histocompatibility complex (MHC) molecules on thymic cortical epithelial cells will survive²⁰. The survived T cells need to go through negative selection in cortical medullary junction later - lots of self-peptides displayed on MHC molecules are here and T cells which show reactivity with them will be deleted²⁰. The remaining T cells will be defined into two categories according to the marker on their surface - either naïve CD4 or naïve CD8 T cell³³. The biggest difference between B cell and T cell is that B cell will become plasma cell and secret antibodies against bacteria or virus, while T cell will release cytokines and directly kill infected or cancer cells¹².

APCs are coming from lymphoid progenitor cells inside bone marrow, and they are like patrolling police officers - they detect infections in our body, take samples such as bacteria antigen, and display on their MHC molecules on their membrane surface, back to nearby lymph nodes, where is the place with high concentration of naïve CD4 and CD8 T cells¹². There are three types of aAPCs: dendritic cell, macrophage, and B cell. All of them can present antigens on their surface with MHC class II molecules and activate CD4 T cells²¹. Antigen presenting cells are especially crucial in adaptive immune response since T cells can only recognize peptide antigens with MHC molecules, which is called peptide-MHC complex, but not recognize antigens in isolated form¹². Especially dendritic cells, they have capability to recognize tumor specific antigens, processing and presenting peptides to naïve CD4 and CD8 T cells which reside in lymph nodes, finally regulating and inducing anti-tumor responses¹². After activation, we call these several T cell types as effector T cells, which proliferate quickly but have a relatively short life.

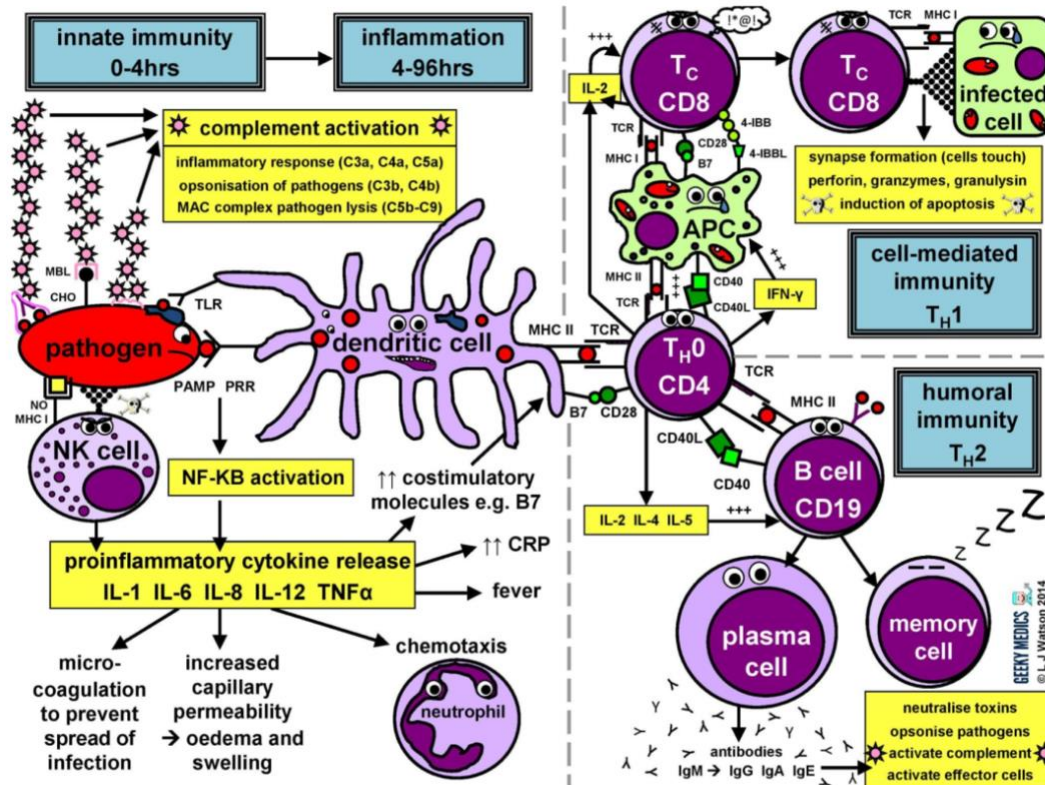


Fig. 1. Overview of immune response. This figure describes the function of immune cells and their signaling pathway⁶³.

There are two pathways that can activate CD8 T cell: one is from infected cell, and the other is from CD4 T cell¹. When the DNA inside the cell is damaged, the cell will be either repaired or destroyed; however, sometimes the damaged cells can find a way to sneak through and keep multiplying out of control, accumulating in a wrong place, thus become tumors or cancer cells over time. Every cells with nucleus have MHC class I on their membrane surface, and the function is to bind the things that produced inside of the cell and display it on the membrane, presenting it out. Our body generates lots of various of CD4 and CD8 positive T cells, which have potential to become helper T cell and cytotoxic T cells respectively, and each of them has different receptors that can recognize a specific antigen²¹. T helper cell will differentiate into T helper cell 1 (Th1) and T helper cell 2 (Th2): Th1 have effect on induction of cell-mediated immunity, and Th2 triggers strong antibody responses². To activate cytotoxic T cell, there are two signals needed: the antigen associates with MHC I complex interacting with T cell receptor (TCR), and co-stimulatory signal - that means the interaction between B7, which is on APC surface and the CD28, which is on T cell surface¹.

The cancer cells usually produce weird proteins inside cell and most of the time, the cytotoxic T cells can recognize the abnormal peptide displayed on MHC I complex and eliminate the cancer cells¹². After forming the immune synapse between cytotoxic T cells and cancer cells, the cytotoxic T cell will release molecules such as perforins, causing holes on the membrane of cancer cells; it could also release granzymes, which can go into the cancer cells and force them to kill themselves¹². The other pathway of activating CD8 T cell is provided by antigen presenting cells. They display antigens on MHC class II and interact with CD4 T cells, activating them and finally lead to Th1 polarization, secreting cytokines such as interferon- γ (IFN- γ) to activate cytotoxic T cells³⁴.

2.2 How artificial cell and stiffness affect immunotherapy

Artificial antigen-presenting cells (aAPCs) has become a promising approach to cancer immunotherapy due to the capability to be precisely controlled in signal delivery, providing reliable and efficient immunomodulation clinical responses in cancer immunotherapy, T cell activation, differentiation, and expansion in vitro³⁶. There are two types of systems for aAPCs -the first one is cell-based, which includes allogenic artificial APCs and xenogeneic artificial APCs; the second is synthetic or exosomal artificial APC systems, which includes polystyrene beads and lipid vesicles, as well as exosomes¹⁶. Most of research using polystyrene beads for both specific and non-specific T cell expansion due to the uniformity of the bead's size and composition, and such approach has lower concern comparing to cell-based aAPCs generated from cell line (meaning coming from cancer cells) when applied to clinical studies. However, it still limits the applications on clinical used because of the possibility of microembolism¹⁶. Nowadays, the focus for aAPCs is to enable T cell persistence after in vitro expansion and adoptive transfer, thus, to establish a long-term immunity for cancer.

Previous studies have demonstrated that T cells are mechano-sensitive, and their activation, differentiation, recognition, and function are regulated by mechanical forces such as contact tension, shear stress, and substrate rigidity^{60,61}. Physical stimuli also influence their gene expression, deformation, organization, and mobility, migration, as well as infiltration altering⁶¹. Mechanical forces are particularly crucial when it comes to regulating the process of T cell antigen recognition, which is a critical step in T cell activation in cell-mediated adaptive immune responses. As a result, substrate stiffness affects T cell activation and should be considered in cancer immunotherapy as well when optimize T cell activation and expansion. Surface receptors such as TCR/MHC trigger a series of cytoskeleton-dependent activities and initiate T cell signaling⁶¹. Throughout the T cell life cycles, they experienced mechanical cues from their surrounding; therefore, some research used elastic material to mimic mechanical microenvironments of tissue or extracellular matrix. Polyacrylamide, poly(dimethylsiloxane), poly(ethylene glycol), alginate, and hyaluronic acid are examples of tunable elasticity systems, which have been a strategy to study external mechanical force and widely used in cell culture⁶¹.

Saitakis M et al., had reported that T cells could migrate longer distances on a stiffer substrate by developing varying stiffness of streptavidin-poly-acrylamide gel coated with biotinylated intercellular adhesion molecules⁶⁰. The protrusions of T cells on higher stiffness substrates are thicker and spread faster comparing to lower stiffness ones, which also implied that T cell morphologies are modulated by substrate stiffness⁶⁰. Further analysis of T cell-specific transcription factors, proliferation transcription factors, surface markers, translation initiation factors, and cytokine productions also shows a positive correlation in response to stiffness⁶⁰. Another investigation on the effect of mechanical stiffness of 3D microenvironment on T cells is reported by Majedi FS et al. The results also show a higher crawling velocity and larger immune synapse of T cells in stiff matrices by establishing an alginate-based hydrogel, which indicates T cells can sense their mechanical 3D environment and discriminate wide range of stiffnesses; thus, here we investigate the effect of stiffness on their functions is worth to investigate⁶².

2.3 Droplet-based Microfluidics

Microfluidics is a systems technology which includes a set of micro-scale channels to achieve a targeted function with control fluid which is geometrically limited. Nowadays, droplet-based microfluidics have been applied to many biomedical applications, such as DNA amplification, cell-based enzymatic assays, high-throughput biochemical assays, and protein crystallization studies³⁰ due to the advantages of high throughput, smaller volume requirement of reagents, and the ability to generate monodispersed droplets. To form the droplet, the two immiscible phases, the dispersed phase and continuous phase, are conducted with different types of channel geometries. The most common geometries include the T junction, flow focusing (cross shape), and co-flowing^{35,40}. In this research, we improve the channel design by incorporating double cross shape structures to generate double emulsion droplets (DED), the droplet encapsulating another droplet³¹.

While the general T-junction devices can be easily fabricated through photolithography, the nonlinear fluidic dynamics could happen due to multiple inflows when parallelizing the T-junction, leading to multimodal or chaotic processes that lead to poor size uniformity of droplets^{56,57}. The flow focusing structure, on the other hand, can precisely control the size and achieve a more stable droplet formation due to the symmetric shearing force of the continuous phase from the outer subchannel⁵¹. The flow focusing technique has been widely used in compound droplet generation and previous studies had reported DED generations in a single step with adjustable droplet size using coaxial flow-focusing devices⁵¹. Theoretically, the axisymmetric flow-focusing device protects wetting at the walls of the outlet channel since it confines droplets in the central axis of the channel⁵³. The co-flow designs are glass-based microfluidics device⁵⁹ and usually, the dispersed phase is injected into another co-flowing immiscible fluid via a needle⁵⁸. They are easier to permeant wettability modification comparing to PDMS devices, reducing the sensitivity to channel wall wetting⁵⁹.

To generate DEDs stably, it is crucial to understand the dynamic behavior of multiphase flows which affects the pressure or rate-of-flow adjustment while applied to the system⁵⁰, especially in the droplet formation processes. Consider a system in the micro-scale, the inertial force is relatively smaller than the viscous force thus there is no interference between different flow layers, resulting in low Reynolds numbers often less than 1³⁵, which is known as the laminar flow, and molecules can be transported in a relatively predictable manner inside microchannels. Capillary number (Ca) is another critical parameter in droplet generation, which is determined by the ratio of viscous to interfacial forces.⁵⁴ Squeezing, dripping, and jetting are three regimes of droplet formation, which are defined by their breakup process⁵². In the squeezing regime, the pressure of upstream built up until the main flow occupied the whole orifice, and the continuous phase squeezes it, driven the breakup occurs within the orifice, which usually happens in low Ca. Dripping, on the other hand, is confined by the geometry. This usually happened in high Ca or high viscosity dispersed phase. The breakup point is just at the exit of the orifice⁵⁰, which caused by shear and surface tension forces acting on the dispersed phase after it goes into the channel⁵⁵. When increasing the flow-rate-ratio (ex. fixed the external phase flow rate and increased internal flow rate), the jetting regime occurs, moving the breakup point to further downstream⁵⁰.

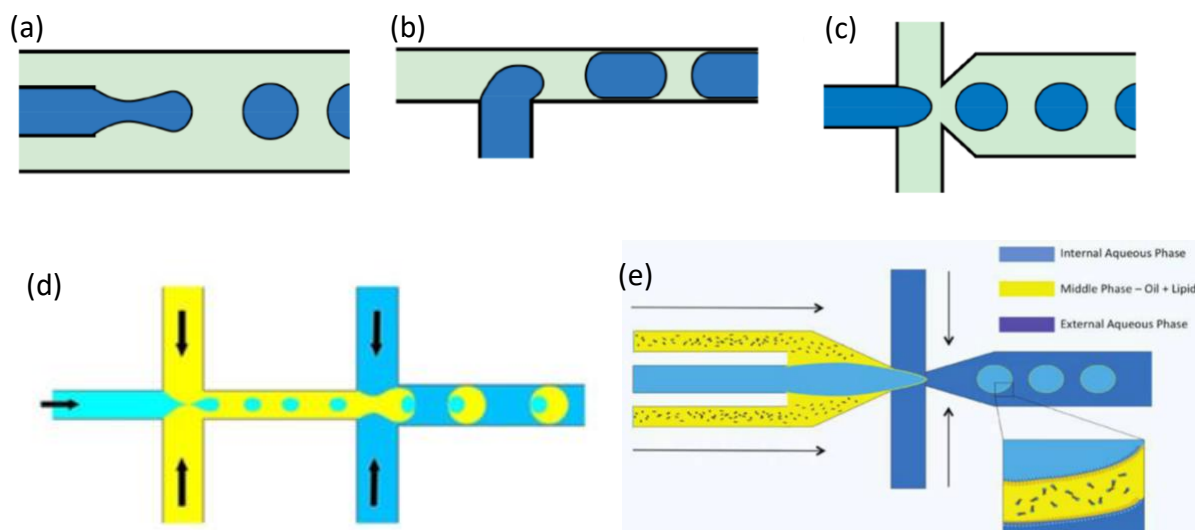


Fig. 2. Schematics images of microfluidic device for most common passive droplet generation method and device for double emulsion droplet generation from Tenje et al.⁴⁰, Chong et al.³¹, and Vallejo et al.²⁴ paper. (a) co-flow⁴⁰. (b) T junction⁴⁰. (c) flow focusing⁴⁰. (d) double cross shape³¹. (e) Flow-focusing²⁴.

2.4 Double emulsion droplet (DED) and artificial cell

Cell membrane plays an important role in biological functions since there are lots of proteins on it, which are used to transport nutrients into cells or acting as a receptor to interact with other cells. The bilayer of the double emulsion droplet is like an artificial membrane: the lipid is in the middle part of the droplet and has a phospholipid bilayer, which is a suitable model for mimicking cell membranes¹⁹. Using microfluidics to generate water-in-oil-in-water (w/o/w) double emulsion microgel droplet with lipid added into oil phase provides an accurate way to synthesize uniform liposomes when comparing to conventional methods such as electroformation, freeze drying, droplet emulsion transfer, hydration, or swelling^{18,28}. The common concepts of artificial cells are in micrometer size and they can have cell-like structure as well as key features of biological cells, or just mimic part of the characteristics of living cells, which were engineered materials without restrictions in structures¹⁹. The dimension of the droplet generated by microfluidic is comparable to the living cell and they have been commonly used in therapeutic applications. The artificial lipid bilayer membranes could be a potential system in drug screening and benefit the study in T cell activation.

For the past decades, microfluidics has become a thriving technology to deal with problems in the emulsification process. Double emulsion droplets, a smaller droplet encapsulated in the other immiscible phase, have been widely applied in industries as food science, cosmetics, pharmaceuticals, biomedical, and agriculture. The two most common cases of double emulsion are oil-in-water-in-oil (o/w/o) emulsion and water-in-oil-in-water (w/o/w) emulsion. The w/o/w droplets have been used in enzyme immobilization, wastewater treatment, and mimicking certain aspects of the living cell to study the properties of biological cells and find potential substitutions for biological cells. The w/o/w droplets have also been reported as potential vehicles for drug delivery, control, and release⁴³ research in single-cell and synthetic biology in the biomedicine field as well, due to its advantages of tunable thickness of each layer, efficient encapsulation, and can be released by temperature or pH change, and other specific triggers^{45,46}.

Due to the low permeability, w/o/w droplets cannot be used as artificial cell-like structures directly, and that makes extracting the excessing solvent in the middle phase the key step to generate cell-sized unilamellar vesicles (CUVs) from double emulsion droplets. Compared to the polymer-composed membranes, the phospholipid bilayers are closer to the texture of natural cell membranes, biocompatible but less stable. For example, the electroformation and reverse emulsification are conventional approaches to generate the giant unilamellar phospholipid vesicles (GUV), the dewetted CUVs, but the size distribution is broad and thus hard to control lipid composition³¹. To achieve monodisperse GUVs generation, Krafft D et al⁴⁹ had reported a method using osmotic gradient with mild centrifuge to form double emulsion droplets fully-dewetted in the eppendorf tube, and it is capable to optimize the oil droplet detachment condition by controlling the flow rate on the dewetting chip.

Surface active agent, which also known as surfactant, plays an important role in double emulsion droplet generation since it affects the size of droplet and encapsulation efficiency, especially when doing long-term stability or storage application such as drug release rate^{30,48}. The surfactant molecule contains a hydrophilic head and a hydrophobic tail. It reduces the surface tension between the two phases by decreasing the density of solvent molecules on the surface⁴⁷. To produce w/o/w emulsion, two surfactants of opposite solubility are needed: a hydrophobic surfactant, which Hydrophilic to Lipophilic Balance (HLB) <10 is dissolved in oil phase such as Span 80, Arlacel P135, as well as Admul Wol 1403, and hydrophilic surfactant (HLB>10) – sodium dodecyl sulphate or synperonic PE/F-68 - needs to be added into aqueous phase⁴³. We can also categorize surfactants into non-ionic and ionic, the later subset includes cationic, anionic, and zwitterionic⁴⁸. The surfactant used in this research is Pluronic F-68 – a hydrophilic surfactant we added in both internal phase and external phase, which is a non-ionic, copolymer detergent widely used in cell culture and is a biological friendly component.

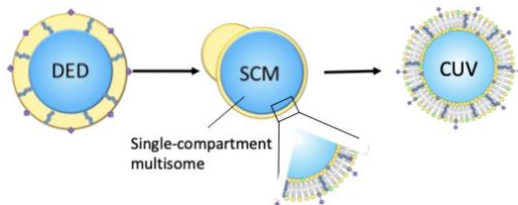


Fig. 3. Schematic of CUV formation from DED

Chapter 3: Research Design and Methods

The goal of this research is to achieve a stable generation of hydrogel DEDs with different stiffnesses for the future use in T cell activation. The PEGDA concentration has been controlled to modulate DED's stiffness. To validate the encapsulation of hydrogel DEDs, we use the Rhodamine (Red) and FITC (Green) dyes to check with the membrane and interior materials. The formed DED will undergo UV light treatment to initiate the crosslinking process. Finally, the DED's stiffness will be tested using the trapping array. In this chapter, we will explain the experiment design, fabrication of DED generation chip, and reagents compositions.

DED Generation
<ul style="list-style-type: none"> • Microchip fabrication • PEGDA concentration modulation (5%-20%) • Encapsulation check with fluorescence • Shelf-life testing

UV Treatment
<ul style="list-style-type: none"> • UV crosslinking • DED survival rate

DED Stiffness Check
<ul style="list-style-type: none"> • Trapping array for DED • Dewetting

3.1 droplet generation device and trapping array

The double emulsion droplet generation device is designed as in Fig. 4. There are three inlets, each representing for the external, oil, internal phases. There are pillars designed to filtrate impurities, avoiding blockage in channels. To minimize the wetting issue, a step structure is set inside the internal phase channel before entering the DED generation region.

The channel heights for internal phase, oil phase, and external phase are 10 μm , 30 μm , and 30 μm respectively, which means there is a 20 μm difference in channel height. The width of internal phase channel is 50 μm , oil phase channel is 30 μm , and 50 μm for external phase channel. (Fig. 4)

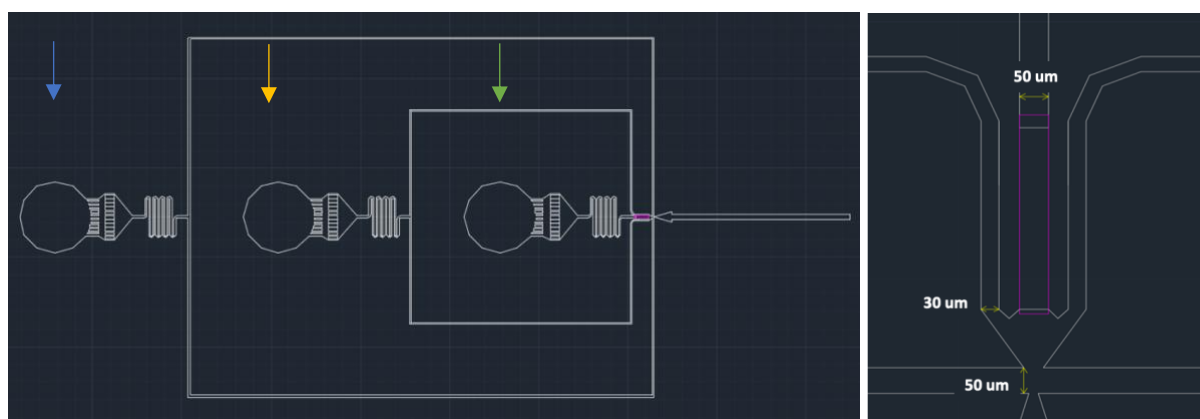
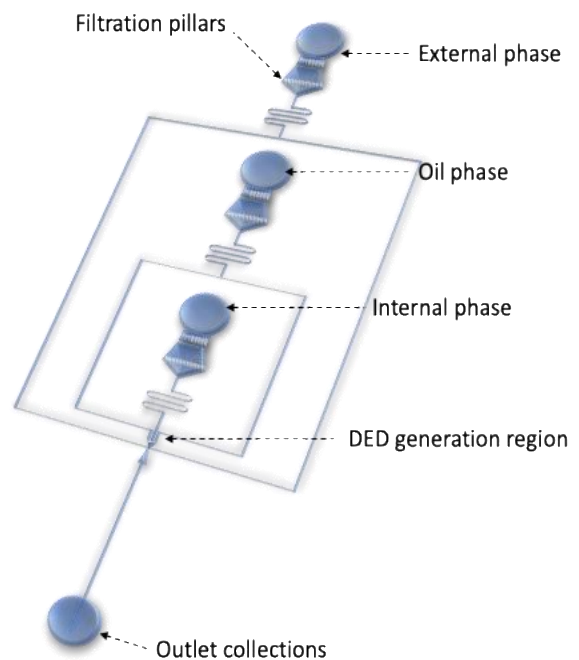


Fig. 4. AutoCAD for microfluidic double emulsion droplet generation chip. (a) Overview design of double emulsion droplet generation device. (b) Zoom in of generation region with step.

To validate that the PEGDA hydrogel inside lipid phase can be crosslinked by UV light, we utilized trapping array (Fig. 5) to catch droplets and observe their deformation under different flow rate. The width x is 0.066 mm, and the gap y is 0.01 mm. After priming by external buffer to remove all air bubbles, we loaded droplets into this device. Due to limited droplets number, we loaded droplets right on the inlet hole instead of using injection mode by syringe pump, which will cause potential droplet loss during pumping. The outlet was connected to the syringe pump applying with the withdraw mode.

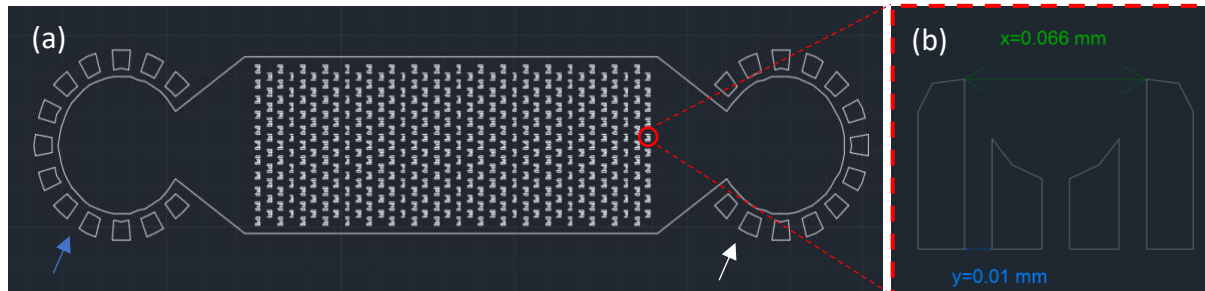


Fig. 5. AutoCAD for microfluidic trapping array. (a) Schematic of trapping array device. The blue arrow is inlet hole loaded with droplets and the white arrow is outlet hole connecting with tubing and syringe pump. (b) Zoom in of the capture region.

3.2 Device fabrication

Both the DED generation chip and the trapping array were fabricated through the photolithography process. First, spin coat SU-8 onto the silicon wafer with an appropriate spin rate for the desired thickness and then put the wafer onto hotplate for the soft bake. The coated wafer was then covered with the photomask for the exposure process to pattern the microstructures. Later, we used the developer solvent to wash off the excess and uncured SU-8. The finalized wafer will be put back to hotplate for the hard bake, to more solidify the structures for downstream uses. After developed the wafer, mixed PDMS monomer and curing agent with 10:1 weight ratio for 2 minutes until we saw it turned white and generated tiny bubbles. Then, poured the PDMS into Petri dish with wafer inside. Put the Petri dish into degasser for 30 minutes and later into the oven with 60 °C overnight. After baking, cut and tear the PDMS from mold, and punch inlets as well as outlet holes. Put PDMS channel and PDMS-coated glass slide into oxygen plasma system and turned on the pump. As soon as the chamber pressure is below 200 psi, starting to adjust the pressure value until it's between 250 to 300 psi. Once the pressure reached to balance, turned the plasma power on for 2 minutes. Bonded PDMS with PDMS-coated glass slide. For the droplet generation microfluidic device, the external phase channel was coated with 0.4% poly(vinyl alcohol) (PVA) for 3 minutes to modify the surface into a more hydrophilic property. A 0.1% PVA was later added to remove the remaining PVA clogging. Lastly, the microchip was put into the oven with 120°C for overnight. All glass slides were washed by the order of isopropanol, DI water, then isopropanol; and the PDMS channels were cleaned by tape to remove dust.

3.3 Reagent composition

The external phase was composed by 30% glycerol, 6% Pluronic F-68, and 125 mM sucrose. The middle oil phase consisted of 1,2-Dioleoyl-*sn*-glycero-3-phosphocholine (DOPC), 1,2-Dipalmitoyl-*sn*-glycero-3-phosphocholine (DPPC), 1,2-distearoyl-*sn*-glycero-3-phosphoethanolamine-N-[biotinyl(polyethylene glycol)-2000] (DSPE-PEG(2000)-biotin), 1,2-dipalmitoyl-*sn*-glycero-3-phosphoethanolamine-N-(lissamine rhodamine B

sulfonyl) (Rhodamine), and cholesterol. The final concentration of the solution for the oil phase was 3:1 volume ratio of DOPC:DPPC, 5 mol% DSPE-PEG(2000), meaning (DOPC mol + DPPC mol)*5%, 0.5 mol% Rhodamine, and 5mg/mL cholesterol. The internal phase were prepared from 250mM sucrose, 1% F-68, 1% wt photoinitiator (2-Hydroxy-4'-(2-hydroxyethoxy)-2-methylpropiophenone), 2mg/mL Fluorescein isothiocyanate (FITC), and Polyethylene (glycol) Diacrylate (PEGDA). To avoid any precipitation caused by undissolved photoinitiator, we centrifuged the internal phase at 10000 RPM for 10 minutes and took only the supernatant before setting up the experiment.

3.4 Experiment setup and parameters

For all experiments, external and oil phase were remained the same while four different concentrations of PEGDA internal phase compositions were tuned to mimic different stiffness of artificial cells and further validated their size, stability, and stiffness variation. We adjusted the PEGDA volume to four different concentrations - 5%, 10%, 15%, 20% - and keeping the rest of the components the same. After droplet generation, the hydrogel droplets from each concentration of were split into two groups, and one of the groups would later be exposed under UV light for 15 minutes to crosslink. Before exposing to the UV light, the droplets were centrifuged with 1000 rpm for 3 minutes and more external phase were added into the vial to dilute the unencapsulated hydrogel, preventing undesired crosslink of hydrogel outside of the droplets.

The three phases of fluids were driven by the pressure pump. We primed all tubing and channels to remove air bubbles right before droplet generation. Based on our experienced, for the pressure adjustment, when increasing the concentration of PEGDA hydrogel, which means the viscosity of internal phase increased, the pressure of the internal phase needs to be decreased since the external phase can cut the internal phase more easily, generating well encapsulated droplets steadily. In general, it is hard to generate PEGDA droplet with high yield constantly with the internal psi over than 1. The whole process was observed under microscope with high-speed camera.

Table 1. Pressure pump setting for 5%, 10%, 15%, and 20% PEGDA hydrogel double emulsion droplet generation.

	5% PEGDA	10% PEGDA	15% PEGDA	20% PEGDA
Internal	1.2~0.8 (psi)	0.77~0.76	0.87~0.77	0.7~0.68
Oil	2.2~2.1	2	2.1	1
External	5~4.5	4~3.3	2.5~2.7	2~2.4

Table 2. Composition of external phase, oil phase, and internal phase, as well as overall experimental condition design. The internal phase composition only showed 5% PEGDA ingredient ration.

External (total=1000 ul)

	stock	add	Final conc.
Glycerol		300 ul	30%
F68	10%	600 ul	6%
NaCl		7.3125 mg	125 mM
H ₂ O		100 ul	

Oil phase (total=1000 ul)

	stock	add	Final conc.
DOPC	50 mg/mL	150 ul	7.5 mg/mL
DPPC	50 mg/mL	50 ul	2.5 mg/mL
DSPE-PEG-biotin 2k	50 mg/mL	39.218595 ul	5 mol%
Rhodamine	10 mg/mL	7.49784 ul	0.5 mol%
Cholesterol		5 mg	5 mg/mL
Oleic acid		753.28 ul	

Internal (total=1000 ul)

	stock	add	Final conc.
PEGDA		50 ul	5%
Sucrose		85.575 mg	250 mM
F68	10%	100	1%
Photoinitiator		10 mg	1 wt%
FITC		2 mg	2 mg/mL
H ₂ O		850 ul	

Experimental design

5%	Biotinylated-lipid	crosslink
10%	Biotinylated-lipid	crosslink
15%	Biotinylated-lipid	crosslink
20%	Biotinylated-lipid	crosslink
5%	Biotinylated-lipid	No crosslink
10%	Biotinylated-lipid	No crosslink
15%	Biotinylated-lipid	No crosslink
20%	Biotinylated-lipid	No crosslink

Chapter 4: Results and Discussion

In this chapter, the results of hydrogel DED generations with different PEDGA concentrations are reported and discussed. Rhodamine and FITC dyes were used to make sure the hydrogel was perfectly encapsulated inside the DEDs. Further investigations of DED's size, stability, and stiffness were also reported.

4.1 Visual detection of hydrogel DED generation

To ensure that droplets are well-generated and did not pop or merge before getting into collecting tubing, the entire process was monitored under a high-speed camera with a microscope. The green reagent in the middle channel is the hydrogel internal phase, the red substance coming from the two channels right next to the internal phase is the oil phase, and the two horizontal channels are the external phase. The Fig 6(a) shows that w/o/w droplets are well-encapsulated. Droplets can be generated up to 12 hours by the syringe pump and the average generation rate is 101 drops/sec. [10 drops*10000 frames per sec/ (5160-4172) frames = 101 drops/sec]. Fig. 6 shows 5% PEGDA generation under the 10X microscope. We have successfully generated 5%, 10%, 15%, 20% hydrogel double emulsion droplets and their configurations are similar to 5%. We also noticed that when increasing the viscosity of internal phase (higher concentration of PEGDA), the generation regime is more likely to change from squeezing to jetting.

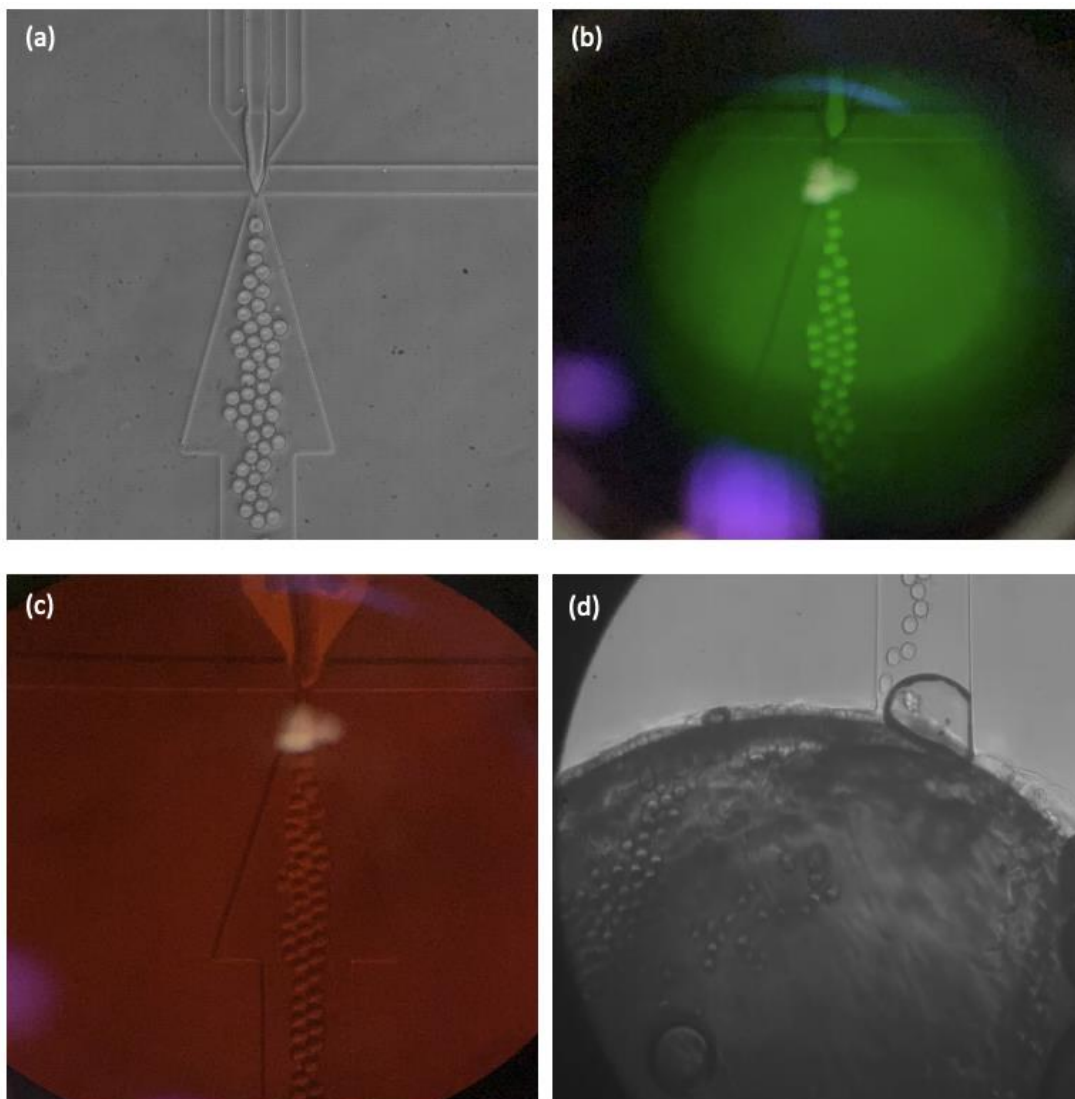


Fig. 6. hydrogel double emulsion droplet generation with 5% PEGDA under 10x microscope (a) bright field (b) green filter for internal phase observation, (c) red filter for oil middle phase observation (d) DED remain unmerged before getting into collecting tubing.

4.2 Hydrogel DED stability, size, and stiffness

(A) Stability

For droplet stability, we compared the droplet concentration decreasing rate of the first week (right after droplet generation) to the fourth week. We pipetted droplets in each collecting vial and did 10X dilution with external buffer and loaded 10ul into hemocytometry to do droplet counting. Table 3 is the one-month decay rate for 5%, 10%, 15%, 20% PEGDA droplets (crosslink and no crosslink). Based on the data, we can roughly conclude that droplet stability may decrease when increasing the hydrogel concentration for both crosslinked and non-crosslinked droplets. All droplets were stored at room temperature. To make sure the droplets are double emulsion encapsulated with hydrogel and to better distinguish the hydrogel and oil droplets, all the counting were measured under the fluorescent microscope. Before exposed to UV light, we centrifuge the droplet with 1000 rpm for 3 minutes and remove partially remove the bottom layer, adding the external phase into it to prevent undesired crosslinks initiates by hydrogel that is not encapsulated well. The starting number of droplets are different since it depends on the entire generation time, and it is hard to mix well by pipetting and diluting to the same concentration; thus, it is more robust to compare their decreasing ratio instead of seeing their numerical value. It is also possible to get measurement error due to not mixing well or potential droplet pop when pipetting it.

For non-crosslinked droplets, as the hydrogel concentration increased, the droplet concentration decreased. We assumed that even when not exposed to UV light, the higher concentration of hydrogel leads to a more viscous inner component, which means stiffer. Consequently, it is not that flexible and would be more likely to pop. It was also interesting to note that there is no significant difference between crosslinked versus non-crosslinked hydrogel droplets. This result is unexpected since after exposure to UV light, hydrogel is supposed to be crosslinked inside and be more stable.

Table 3. Crosslinked and non-crosslinked hydrogel DED stability.

1st repeat

week	5% crosslink	10% crosslink	15% crosslink	20% crosslink
1	100000	10000	150000	20000
4	72500	5000	47500	10000
Decreasing ratio	0.275	0.5	0.68	0.5

week	5% no crosslink	10% no crosslink	15% no crosslink	20% no crosslink
1	160000	25000	100000	52500
4	128000	15000	50000	13000
Decreasing ratio	0.2	0.4	0.5	0.75

2nd repeat

week	5% crosslink	10% crosslink	15% crosslink	20% crosslink
1	10000	138000	128000	153000
4	13000	57500	57500	32500
Decreasing ratio	N/A	0.58	0.55	0.79

week	5% no crosslink	10% no crosslink	15% no crosslink	20% no crosslink
1	25000	133000	77500	113000
4	7500	90000	168000	55000
Decreasing ratio	0.7	0.32	N/A	0.51

(B) Size

After generating hydrogel double emulsion droplets, we put them into hemocytometry and took images under fluorescent microscope. Red dots are oil droplets only and green dots encapsulated by red circles are double emulsion droplets. The droplet size is about 20 to 25 μm . Below are the images taken before and after droplets exposed to UV light for 15 minutes. According to the data, we can see that UV light does not affect hydrogel DED size and their configuration.

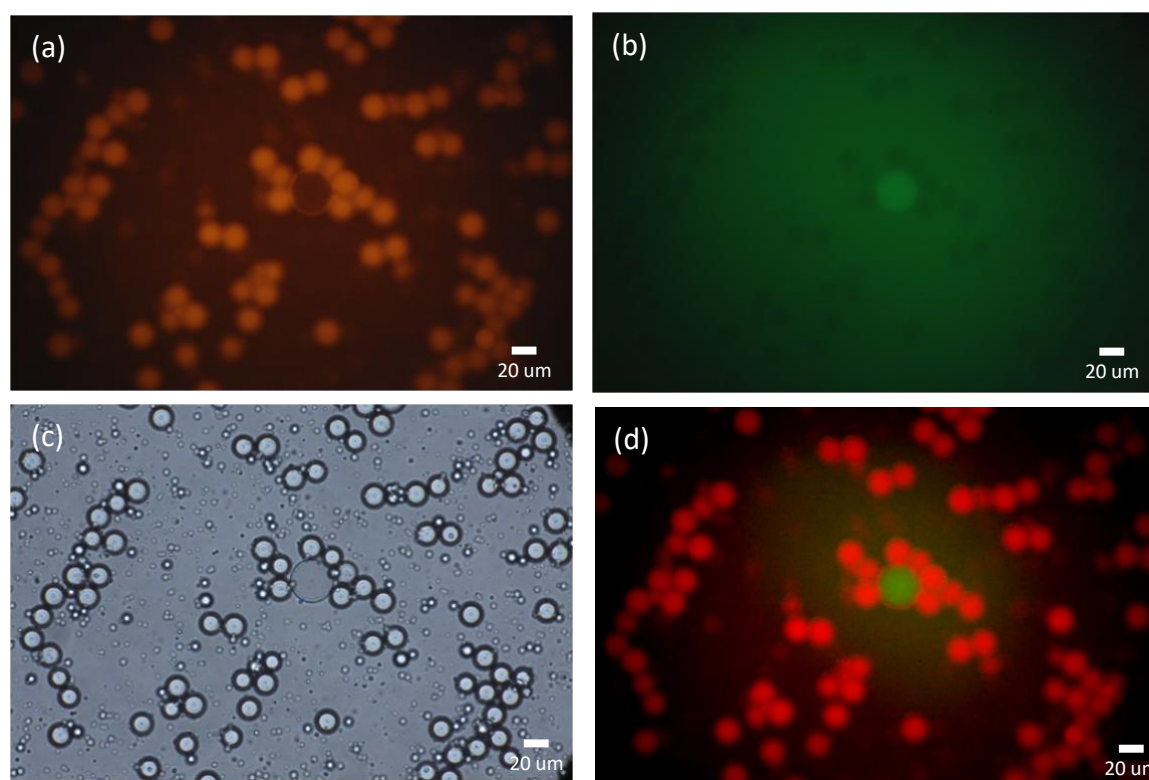


Fig. 7. 5% PEGDA DED before exposed to UV and imaged under 40X microscope. (a) red filter. (b) green filter. (c) bright field. (d) merge figure.

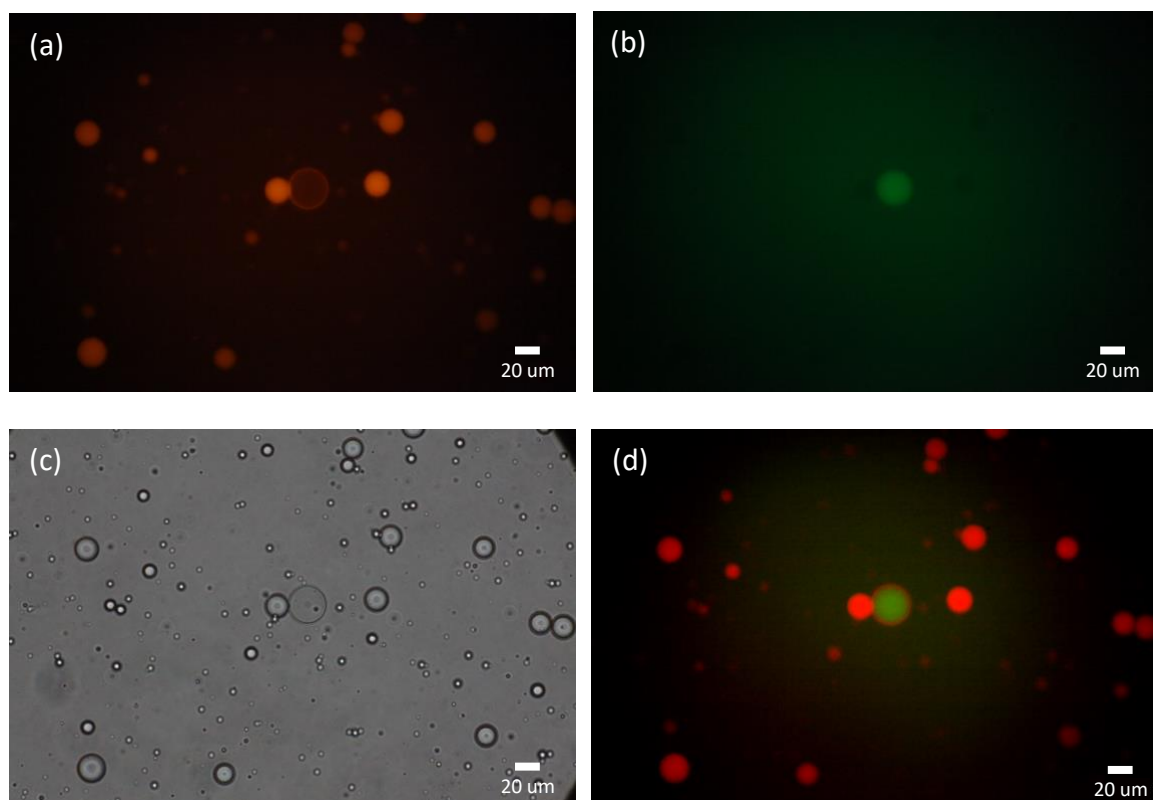


Fig. 8. 5% PEGDA DEDs after exposed to UV light and imaged under 40X microscope.

Also, since the droplets will be incubated with PBMC cells after conjugating antigens on their lipid bilayer, it is valuable to check whether they can maintain their structure while in the culture medium for PBMC cells. We added hydrogel droplets into RPMI culture medium and below are the pictures before and after hydrogel DEDs added into medium. The droplet size did not change significantly, the internal phase did not leak out, and droplets did not shrink and still maintain their shape when observed under fluorescent microscope. However, when detecting under bright field, we can see some wrinkle-like structure on it, and the lipid-oil shell seems a little distorted. We hypothesized there is interaction between RPMI and oil-lipid phase. In order to validate this hypothesis, our collaborator Becky Chen added oleic acid drops in RPMI. It turned out that she saw the wrinkles on oleic acid drops.

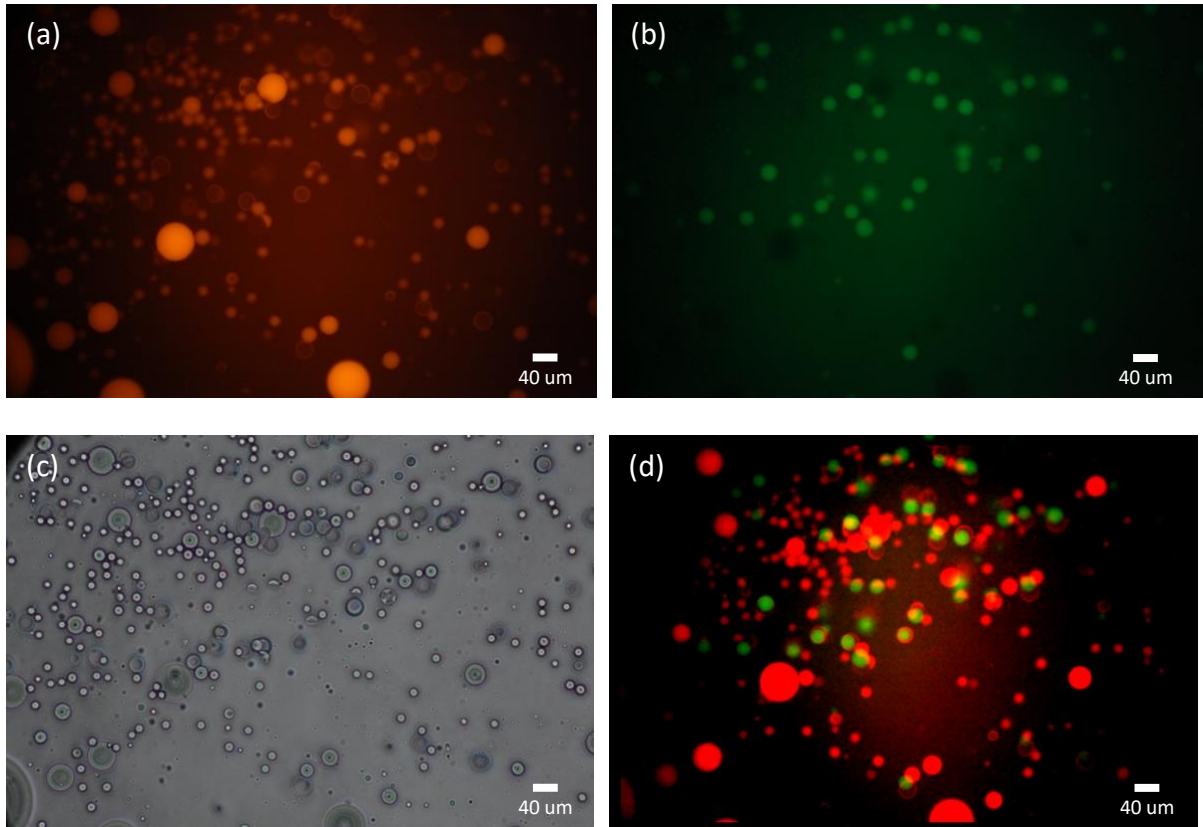


Fig. 9. 5% PEGDA non-crosslinked DEDs before adding RPMI under 20X microscope.

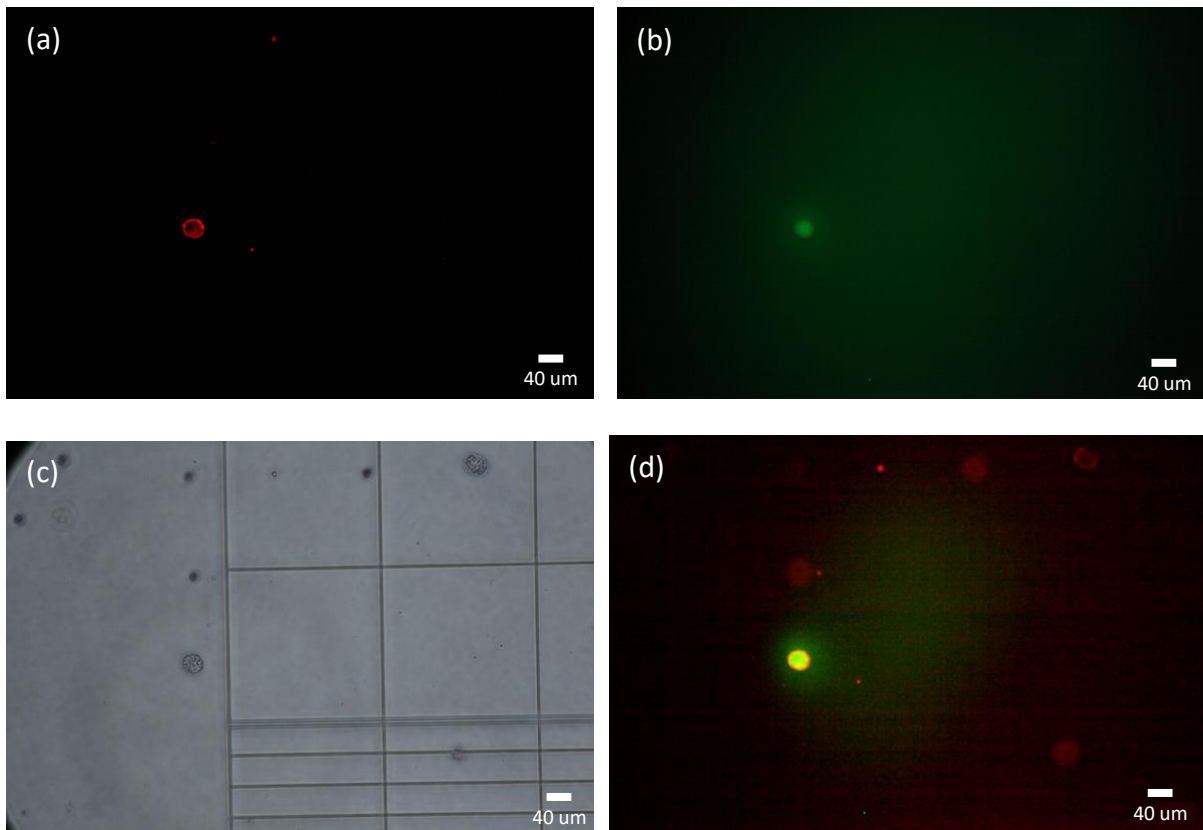


Fig. 10. 5% PEGDA no crosslinked DED after adding RPMI under 20X microscope.

(C) Droplet stiffness

To validate that the lipid and oil phase do not block UV light and the hydrogel inside lipid bilayer can still be crosslinked, we used trapping array to catch hydrogel droplets and see the time consumed by crosslinked as well as non-crosslinked hydrogel droplets to squeeze through the gap between ridges. The entire process was recorded by video under 20X microscope and the figures below are the screen shots of different timing from video. As shown in figure, before exposed under 15 minutes UV light, 5% PEGDA droplets were trapped without any deformation. A withdraw flow rate of 5 ul/min and 10 ul/min was assigned to the outlet of the channel for this stiffness testing. The droplets without being exposed by UV light squeezed through the gap within 1 min under 10 ul/min flow rate; nevertheless, the droplets can last for 75 seconds, which means 20 more seconds, after treating with UV light.

We also noticed that this device would be an ideal tool for dewetting as long as the flow rate is high enough. The crosslinked hydrogel droplets cannot even be dewetted under the flow rate of 5 ul/min and the droplets did not go through the gap even they have deformed to some extent. As shown in Fig. 13, the crosslinked droplets last for more than 80 seconds when under 5 ul/min flow rate. After increasing the flow rate up to 10 ul/min (Fig. 14), we saw the droplets can be dewetted within 20 seconds, leaving the rest part of the CUVs unimpaired. Even though non-crosslinked droplets can be partially dewetted to single compartment multisomes (SCMs), it is still difficult to deplete oil drop completely from it without any damage. This dewetting method is more suitable applying to crosslinked hydrogel droplets than in non-crosslinked one since the non-crosslinked droplets are too soft to maintain their structure and separate from the oil drop.

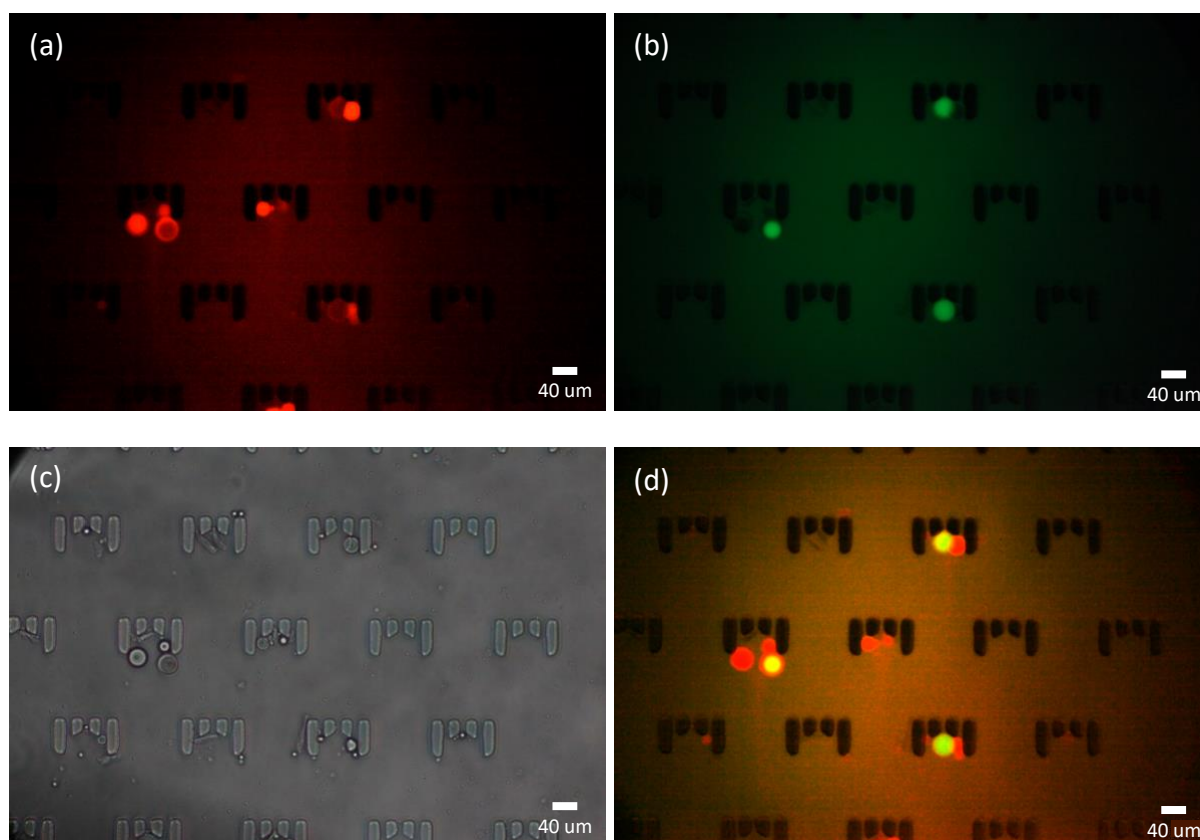


Fig. 11. 5% PEGDA DED before UV under 20x microscope. After priming, we stopped the flow and ensured DEDs were trapped without complete dewet.

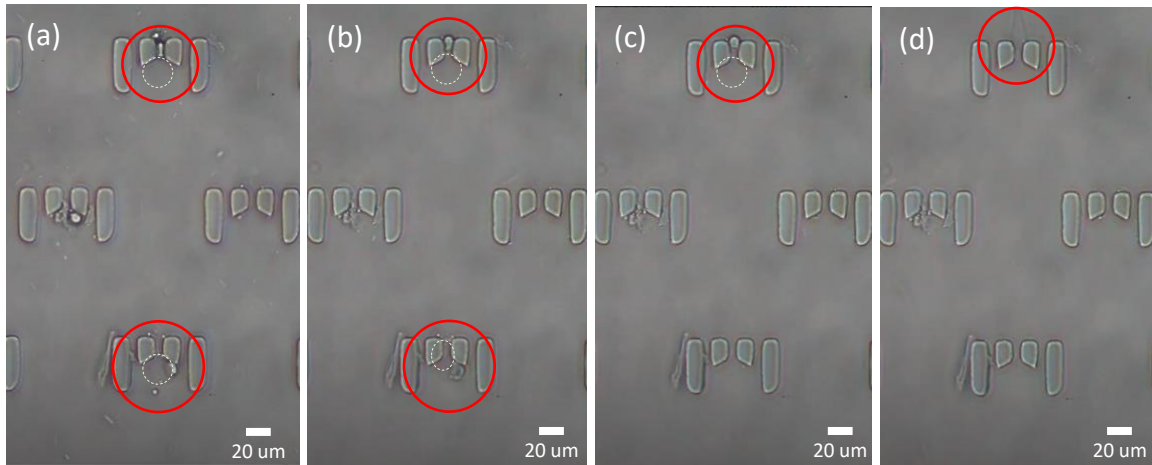


Fig. 12. Screen shot from video of 5% PEGDA DED before UV under 20x microscope with flow rate = 10 ul/min. After pulling (a) 5 second (b) 46 second (c) 52 second (d) 53 second. Under this flow rate, hydrogel SCM is difficult to separate from the oil cap. The white circles indicate the positions of DEDs since they are hard to be seen under the bright field.

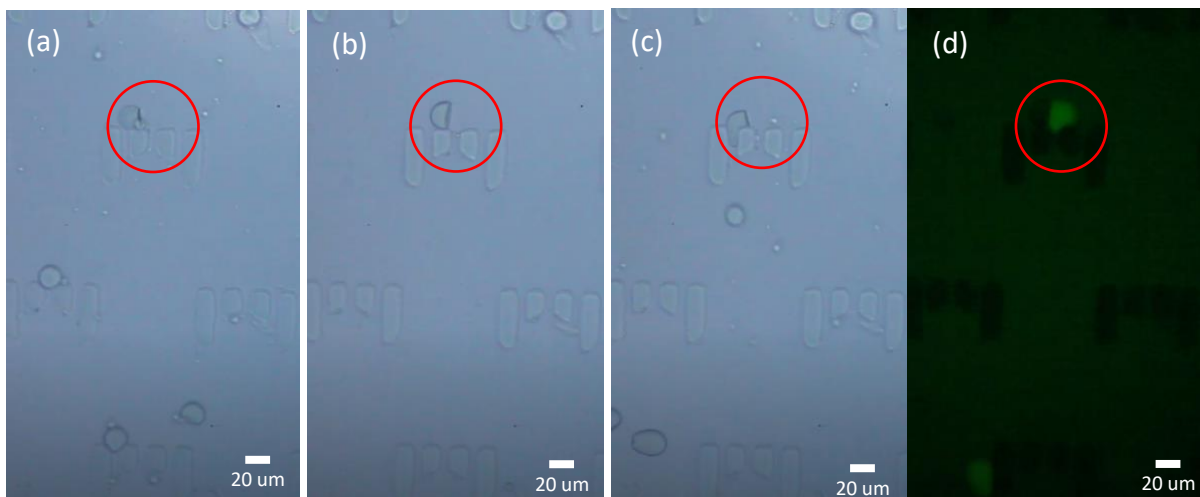


Fig. 13. Screen shot from video of 5% PEGDA DED after UV under 20x microscope with flow rate = 5 ul/min. After pulling (a) 2 second (b) 17 second (c) 35 second (d) 82 second. When under this flow rate, we saw the partially deformation of hydrogel SCM, but it cannot either squeeze through the gap or dewet completely even over 80 second.

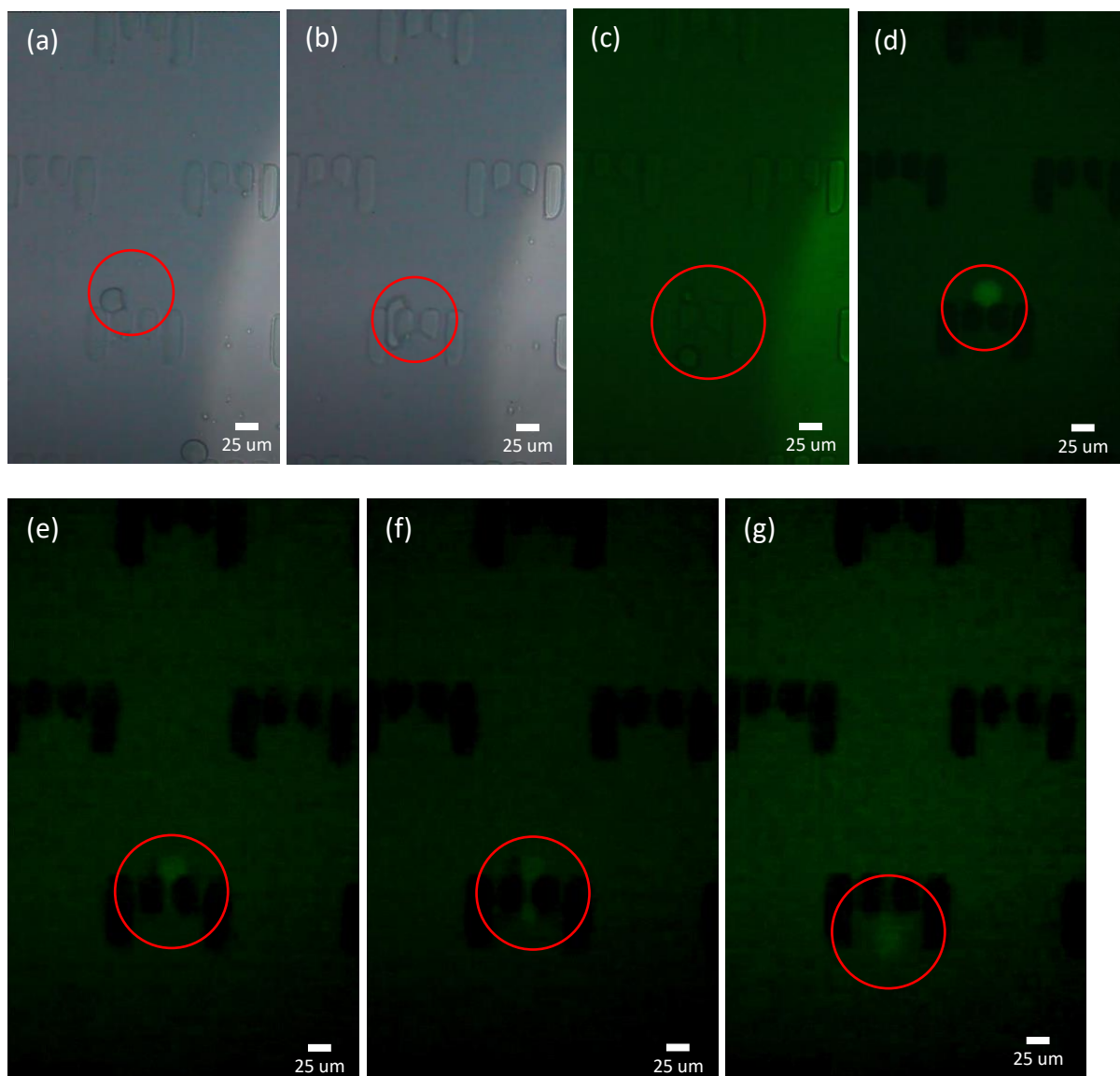


Fig. 14. Screen shot from video of 5% PEGDA DED after UV under 20x microscope with flow rate = 10 $\mu\text{l}/\text{min}$. After pulling (a) 8 second (b) 16 second (c) 17 second (d) 20 second (e) 75 second (f) 75.5 second (g) 76 second. After withdrawing for 16 seconds under this flow rate, it started to dewet, and the oil cap detached with the hydrogel droplet at 17th second. The hydrogel droplet was crosslink and took more than one minutes to squeeze through the gap.

Chapter 5: conclusion

5.1 Discussion of results

In summary, this research provides a new concept to mimic antigen presenting cell: tunable stiffness with fluidity artificial membrane. We demonstrated promising methods for hydrogel double emulsion droplet (DED) generation and stiffness validation as well as dewetting by microfluidics. Even under microscale and encapsulated inside lipid, PEGDA can still be crosslinked, and their variance of stiffness depend on hydrogel concentration. Moreover, with the biotinylated lipid, droplets can be conjugated with antibodies and antigens by biotin-streptavidin interaction. Based on the collaborator, Becky Chen, we already confirmed the regular w/o/w DEDs can interact with cells and it is capable to do cytokine evaluation; however the interaction of hydrogel DEDs with cells and cytokine evaluation should be further tested since the cells survival rate was too low to do the examination.

There are several details we must know during droplet generation. For device fabrication, it is important to seal the tubing with lead completely with hot-melt adhesive (hot glue gun loaded with a glue stick); otherwise, the internal phase will seem more viscous and pressure pump may not work well, fail to form droplets. In addition, sometimes the pressure is not stable, thus it is also suitable to use syringe pump for 5% PEGDA internal phase; the range of flow rate is between 0.14 ul/min to 0.2 ul/min. We successfully generated 5% PEGDA DEDs for up to 12 hours by syringe pump; however, since the flow rate needs to be lower when generating higher concentration hydrogel droplets, it may be not applicable to our syringe pump to reach the flow rate below 0.1 ul/min accurately. Furthermore, lower the oil phase as much as we can help to mimic lipid bilayer more successfully; therefore, it is proper to find the critical point for the oil pressure, control the thickness of middle phase precisely, not merely adjust the pressure to droplet formation. Too much oil may cause DEDs merge together easily. There is also a clogging issue that might happened in the channel of internal phase after generating droplets for a long period of time, which is caused from the slight backflow of oil to the internal phase channel. Increasing the oil phase pressure and let it first flows into internal phase channel, then decreasing it rapidly can flush away the oil in internal phase channel and alleviate such problem.

Although we roughly got the data for droplet stability, number of droplets measured by hemocytometry is not concrete enough due to inevitable human measurement error, and we still did not find an appropriate explanation to justify the increased decay ratio for those crosslinked hydrogel droplets in higher concentration. One possibility would be that FITC decay very quickly, and we used green filter only when observed droplets, thus after UV exposure and even under fluorescent light for merely a few minutes, we may not detect it. We hypothesized that UV light damages FITC, and such phenomenon was discovered in collecting vial as well – the content color in the vial turned from light green to more transparency after UV treatment. The other potential reason may be not fully crosslink of the DED.

In addition, despite having no reports on cell toxicity for all these materials, it seems that sometimes the survival rate of cells decreased significantly when incubated PBMC cells with double emulsion droplets – either hydrogel double emulsion droplet or regular water-in-oil-in-water droplet. This research collaborated with Becky Chen and according to her research, the cell survival rate is even lower than incubated cells with tetanus or NYESO free molecules or bead. This will lead to the difficulty in further cytokines evaluation by ELISA and flow cytometry since we do not have enough cells. To figure out which composition in the droplets

causes toxicity to cells, we cultured cells into different solutions and the result revealed that oil plus lipid seems to be the main factor causes cell death.

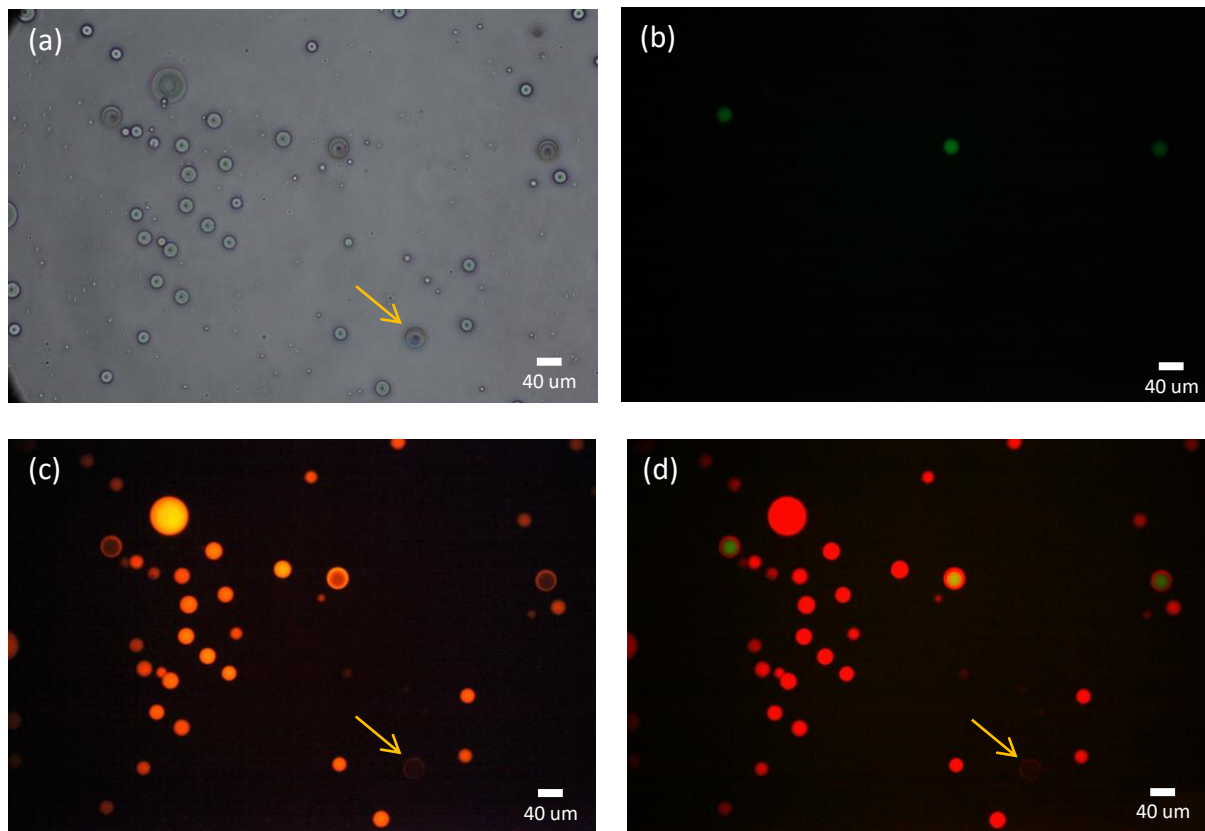


Fig. 15. Example of 5% PEGDA DED after UV under 20x microscope. In figure (a), (c), and (d) we can see the droplet; however, in figure (b) under green filter, we did not see the specific droplet. This indicated the fast decay of FITC caused measurement error.

5.2 Limitation of the study

Due to time and budget constrain, it is difficult to observe droplet stability for a longer period. Additionally, we only demonstrated that 5% PEGDA hydrogel double emulsion droplets can be crosslinked when exposed by UV light; however, 10%, 15%, and 20% PEGDA hydrogel droplets still need to be validated. Instead of utilizing trapping array, using AFM to test their stiffness will be an idea tool to get a numerical number, which can be more solid and easier when doing stiffness study, and further validating that different concentration of PEGDA hydrogel droplets have different stiffness after being exposed by UV light in microscale.

Separating oil droplets with hydrogel droplets would be another issue since when using trapping array, the oil droplets occupied the capture regions, preventing hydrogel droplets to be well-trapped. We tried to centrifuge hydrogel droplets with 1000 rpm for 3 minutes after droplet generation, but the oil droplets float up to the top layer as well and both of them accumulated in the same layer. Higher spin speed may break hydrogel droplets thus it is not acceptable. This would also cause bias when incubating droplets with cells if part of the cells interacted with antigens on oil droplets instead of double emulsion droplets.

Hydrogel droplets may float up to the surface after stored for a while, and this phenomenon appeared when incubating droplets with PBMCs as well. The cells would sink to the bottom while droplets float up, such situation may reduce the interaction between cells and hydrogel

droplets. Even though we still detected the interaction between cells and double emulsion droplets, it is very rare and the activation level is not as high as expected. We tried to encapsulate 5 nm magnetic beads inside droplets by adding them into internal phase. However, it seems that the encapsulation efficiency is low and after few hours later, we can see precipitation caused by beads in both collecting vial and syringe. Improving the contact between cells and droplets would be the other issue we need to overcome.

Lastly, stabilizing the CUV is also a problem since the double emulsion droplets seems to pop easily after dewetting in 2x PBS + 50% glycerol. We tried other composition for dewetting solution; nevertheless, double emulsion droplets may dewet to SCM instead of completely dewet to CUV when transferring into either 1x PBS or 2x PBS. We already validated that it is appropriate to use trapping array helping deplete the oil but the lifespan of CUV needs to be further observed and verified.

5.3 Future directions

This research mainly focuses on PEGDA hydrogel double emulsion droplet generation and stiffness examination, which are only the first step in T cell activation optimization in immunotherapy research and there are several obstacles still need to be overcome. Wetting, which means the internal phase sticks to generation region, is one issue during the double emulsion droplet generation since once it sticks on the channel, it is impossible for it to go back to the balance automatically, thus we need to be like a babysitter, keep monitoring and adjusting the pressure manually to find another equilibrium again. While Becky optimized the channel by adding a step into internal phase channel and our flow-focusing geometry possibly thinner the oil in the middle phase, we already demonstrated that double emulsion droplets can be dewetted by either squeezing channel or trapping array; therefore, it is still worthy to try to change the geometry to double T junction, which may help to reduce the wetting issue potentially.

Furthermore, the double emulsion droplets seem shrink when we put them into RPMI, which is the culture medium for T cell. Even though the droplets are not popped, and the cells can still be activated with the shrink droplets, there may have some interaction between RPMI and the oil phase. Increasing cell survival rate is relative to our middle phase composition as well; thus, try to use different material, filter the oil, or decreasing lipid concentration would be a potential method to solve these problems.

Oil and hydrogel droplet isolation device can be future improved. Some research already demonstrated that microfluidics could do cell sorting based on their stiffness difference³². We assumed that by using the cell sorting device shown below, it is possible to isolate most of the oil droplets from double emulsion droplets, as well as verifying stiffness difference between various concentration hydrogel droplets after UV exposure.

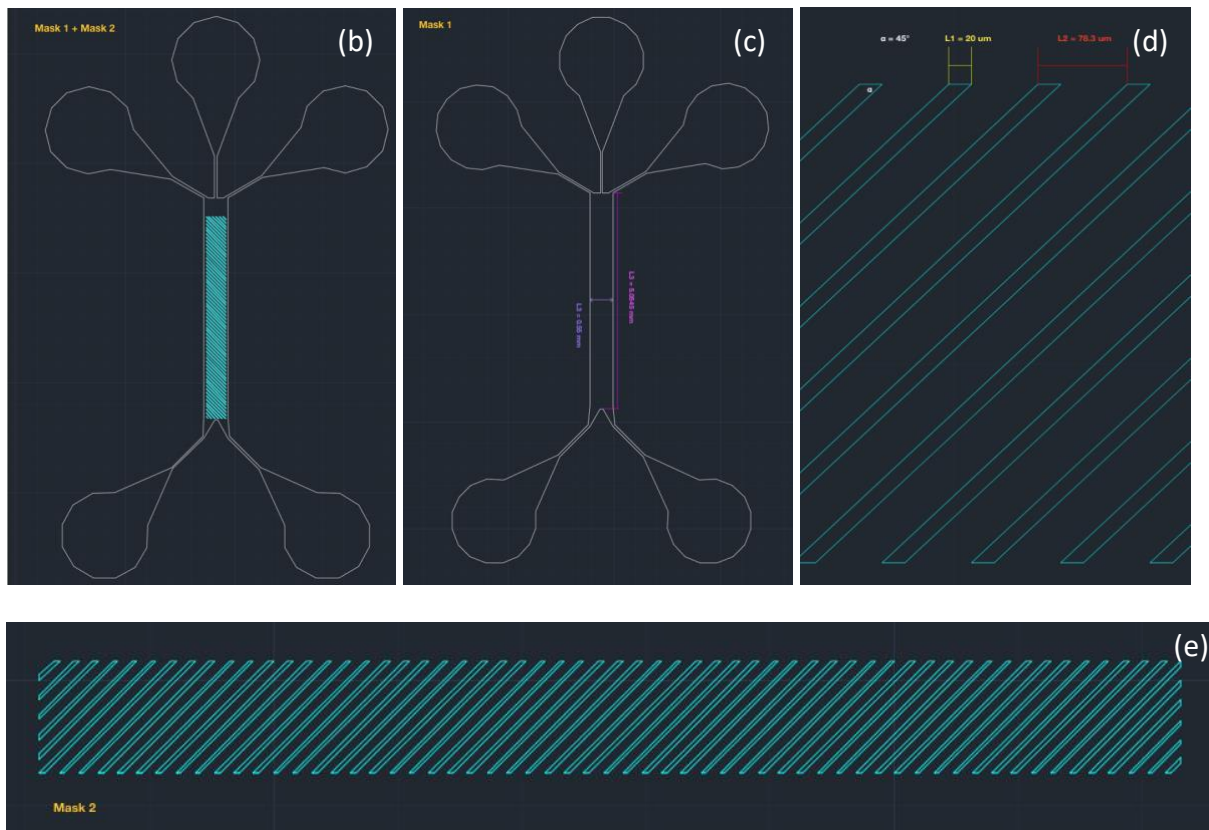
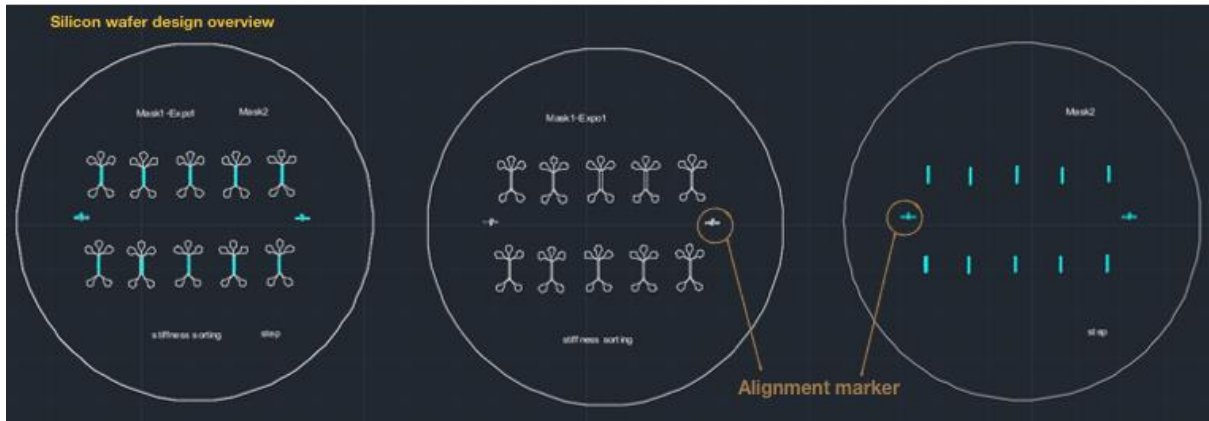


Fig. 16. Microfluidic design for stiffness sorting. Microfluidics molds are fabricated with negative photoresist SU-8 and then soft lithography with Polydimethylsiloxane (PDMS). The design of microfluidic photomask were made on AutoCAD software and "1" inside indicates 1 mm and the mold was produced on a 3" silicon wafer. In order to fabricate pillars on the top inside of the channel, we need to design two masks since there are two different heights in this device. Both masks are emulsion down with black background, and the white area on the mask will be exposed under UV, which indicates the area will crosslink. On the other hand, the black area on the mask will not be exposed under UV, thus those area will be wash away by solvent. The channel height needs to be adjusted according to the droplets we are going to categorize, thus in this research the channel height is 20 μm .

Chapter 6: References

1. Zhang, S., Zhang, H., & Zhao, J. (2009). *The role of CD4 T cell help for CD8 CTL activation. Biochemical and Biophysical Research Communications*, 384(4), 405–408. doi:10.1016/j.bbrc.2009.04.134
2. Lanzavecchia A, Sallusto F. Progressive differentiation and selection of the fittest in the immune response. *Nat Rev Immunol*. 2002 Dec;2(12):982-7. doi: 10.1038/nri959.
3. A. Ayoib, U. Hashim, M. K. M. Arshad and V. Thivina, "Soft lithography of microfluidics channels using SU-8 mould on glass substrate for low cost fabrication," *2016 IEEE EMBS Conference on Biomedical Engineering and Sciences (IECBES)*, 2016, pp. 226-229, doi: 10.1109/IECBES.2016.7843447.
4. Kamiya, K., & Takeuchi, S. (2017). *Giant liposome formation toward the synthesis of well-defined artificial cells. Journal of Materials Chemistry B*, 5(30), 5911–5923. doi:10.1039/c7tb01322a
5. van Gisbergen KP, Aarnoudse CA, Meijer GA, Geijtenbeek TB, van Kooyk Y. Dendritic cells recognize tumor-specific glycosylation of carcinoembryonic antigen on colorectal cancer cells through dendritic cell-specific intercellular adhesion molecule-3-grabbing nonintegrin. *Cancer Res*. 2005;65(13):5935-5944. doi:10.1158/0008-5472.CAN-04-4140
6. Siegel, R.L., Miller, K.D. and Jemal, A. (2019), Cancer statistics, 2019. *CA A Cancer J Clin*, 69: 7-34. <https://doi.org/10.3322/caac.21551>
7. Chakraborty S, Rahman T. The difficulties in cancer treatment. *Ecancermedicalscience*. 2012;6:ed16. Published 2012 Nov 14. doi:10.3332/ecancer.2012.ed16
8. Arruebo M, Vilaboa N, Sáez-Gutierrez B, et al. Assessment of the evolution of cancer treatment therapies. *Cancers (Basel)*. 2011;3(3):3279-3330. Published 2011 Aug 12. doi:10.3390/cancers3033279
9. Utada, A. S. (2005). *Monodisperse Double Emulsions Generated from a Microcapillary Device. Science*, 308(5721), 537–541. doi:10.1126/science.1109164
10. Zhang, D.K.Y., Cheung, A.S. & Mooney, D.J. Activation and expansion of human T cells using artificial antigen-presenting cell scaffolds. *Nat Protoc* **15**, 773–798 (2020). <https://doi.org/10.1038/s41596-019-0249-0>
11. Lugano, R., Ramachandran, M. & Dimberg, A. Tumor angiogenesis: causes, consequences, challenges and opportunities. *Cell. Mol. Life Sci.* **77**, 1745–1770 (2020). <https://doi.org/10.1007/s00018-019-03351-7>
12. Gonzalez H, Hagerling C, Werb Z. Roles of the immune system in cancer: from tumor initiation to metastatic progression. *Genes Dev*. 2018;32(19-20):1267-1284. doi:10.1101/gad.314617.118
13. Jardim DL, Groves ES, Breitfeld PP, Kurzrock R. Factors associated with failure of oncology drugs in late-stage clinical development: A systematic review. *Cancer Treat Rev*. 2017;52:12-21. doi:10.1016/j.ctrv.2016.10.009
14. Chui PL. Cancer- and Chemotherapy-Related Symptoms and the Use of Complementary and Alternative Medicine. *Asia Pac J Oncol Nurs*. 2019;6(1):4-6. doi:10.4103/apjon.apjon_51_18
15. Majedi, F. S., Hasani-Sadrabadi, M. M., Thauland, T. J., Li, S., Bouchard, L.-S., & Butte, M. J. (2020). *T-cell activation is modulated by the 3D mechanical microenvironment. Biomaterials*, 120058. doi:10.1016/j.biomaterials.2020.120058

16. Turtle CJ, Riddell SR. Artificial antigen-presenting cells for use in adoptive immunotherapy. *Cancer J*. 2010;16(4):374-381. doi:10.1097/PPO.0b013e3181eb33a6
17. Stanculeanu DL, Daniela Z, Lazescu A, Bunghez R, Anghel R. Development of new immunotherapy treatments in different cancer types. *J Med Life*. 2016;9(3):240-248.
18. Supramaniam P, Ces O, Salehi-Reyhani A. Microfluidics for Artificial Life: Techniques for Bottom-Up Synthetic Biology. *Micromachines (Basel)*. 2019;10(5):299. Published 2019 Apr 30. doi:10.3390/mi10050299
19. Xu C, Hu S, Chen X. Artificial cells: from basic science to applications. *Mater Today (Kidlington)*. 2016;19(9):516-532. doi:10.1016/j.mattod.2016.02.020
20. Klein L, Kyewski B, Allen PM, Hogquist KA. Positive and negative selection of the T cell repertoire: what thymocytes see (and don't see). *Nat Rev Immunol*. 2014;14(6):377-391. doi:10.1038/nri3667
21. Marshall JS, Warrington R, Watson W, Kim HL. An introduction to immunology and immunopathology. *Allergy Asthma Clin Immunol*. 2018;14(Suppl 2):49. Published 2018 Sep 12. doi:10.1186/s13223-018-0278-1
22. Dimberu PM, Leonhardt RM. Cancer immunotherapy takes a multi-faceted approach to kick the immune system into gear. *Yale J Biol Med*. 2011;84(4):371-380.
23. Larsen, J. N., Broge, L., & Jacobi, H. (2016). *Allergy immunotherapy: the future of allergy treatment*. *Drug Discovery Today*, 21(1), 26–37. doi:10.1016/j.drudis.2015.07.010
24. Vallejo D, Lee SH, Lee D, et al. Cell-sized lipid vesicles for cell-cell synaptic therapies. *Technology (Singap World Sci)*. 2017;5(4):201-213. doi:10.1142/S233954781750011X
25. Houot, R., Schultz, L. M., Marabelle, A., & Kohrt, H. (2015). *T-cell-based Immunotherapy: Adoptive Cell Transfer and Checkpoint Inhibition*. *Cancer Immunology Research*, 3(10), 1115–1122. doi:10.1158/2326-6066.cir-15-0190
26. Hayes, C. Cellular immunotherapies for cancer. *Ir J Med Sci* **190**, 41–57 (2021). <https://doi.org/10.1007/s11845-020-02264-w>
27. Cintolo JA, Datta J, Mathew SJ, Czerniecki BJ. Dendritic cell-based vaccines: barriers and opportunities. *Future Oncol*. 2012;8(10):1273-1299. doi:10.2217/fon.12.125
28. Deng, N.-N., Yelleswarapu, M., & Huck, W. T. S. (2016). *Monodisperse Uni- and Multicompartment Liposomes*. *Journal of the American Chemical Society*, 138(24), 7584–7591. doi:10.1021/jacs.6b02107
29. Eggermont LJ, Paulis LE, Tel J, Figdor CG. Towards efficient cancer immunotherapy: advances in developing artificial antigen-presenting cells. *Trends Biotechnol*. 2014;32(9):456-465. doi:10.1016/j.tibtech.2014.06.007
30. Martino, C., & deMello, A. J. (2016). *Droplet-based microfluidics for artificial cell generation: a brief review*. *Interface Focus*, 6(4), 20160011. doi:10.1098/rsfs.2016.0011
31. Chong, D., Liu, X., Ma, H., Huang, G., Han, Y. L., Cui, X., ... Xu, F. (2015). *Advances in fabricating double-emulsion droplets and their biomedical applications*. *Microfluidics and Nanofluidics*, 19(5), 1071–1090. doi:10.1007/s10404-015-1635-8
32. Wang, G., Mao, W., Byler, R., Patel, K., Henegar, C., Alexeev, A., & Sulchek, T. (2013). *Stiffness Dependent Separation of Cells in a Microfluidic Device*. *PLoS ONE*, 8(10), e75901. doi:10.1371/journal.pone.0075901

33. Starr, T. K., Jameson, S. C., & Hogquist, K. A. (2003). *POSITIVE AND NEGATIVE SELECTION OF T CELLS*. *Annual Review of Immunology*, 21(1), 139–176. doi:10.1146/annurev.immunol.21.120601.141107
34. Alberts B, Johnson A, Lewis J, et al. *Molecular Biology of the Cell*. 4th edition. New York: Garland Science; 2002. Helper T Cells and Lymphocyte Activation. Available from: <https://www.ncbi.nlm.nih.gov/books/NBK26827/>
35. Zhu, P., & Wang, L. (2017). Passive and active droplet generation with microfluidics: a review. *Lab on a Chip*, 17(1), 34–75. doi:10.1039/c6lc01018k
36. Eggermont LJ, Paulis LE, Tel J, Figdor CG. Towards efficient cancer immunotherapy: advances in developing artificial antigen-presenting cells. *Trends Biotechnol.* 2014;32(9):456-465. doi:10.1016/j.tibtech.2014.06.007
37. Zhu, Y., & Fang, Q. (2013). *Analytical detection techniques for droplet microfluidics—A review*. *Analytica Chimica Acta*, 787, 24–35. doi:10.1016/j.aca.2013.04.064
38. Cui, P., & Wang, S. (2018). *Applications of microfluidic chip technology in pharmaceutical analysis: A review*. *Journal of Pharmaceutical Analysis*. doi:10.1016/j.jpha.2018.12.001
39. Teh, S.-Y., Lin, R., Hung, L.-H., & Lee, A. P. (2008). *Droplet microfluidics*. *Lab on a Chip*, 8(2), 198. doi:10.1039/b715524g
40. Tenje, M., Fornell, A., Ohlin, M., & Nilsson, J. (2017). *Particle Manipulation Methods in Droplet Microfluidics*. *Analytical Chemistry*, 90(3), 1434–1443. doi:10.1021/acs.analchem.7b01333
41. Scott SM, Ali Z. Fabrication Methods for Microfluidic Devices: An Overview. *Micromachines*. 2021; 12(3):319. <https://doi.org/10.3390/mi12030319>
42. Kane, R. S., Stroock, A. D., Li Jeon, N., Ingber, D. E., & Whitesides, G. M. (2002). *Soft Lithography and Microfluidics*. *Optical Biosensors*, 571–595. doi:10.1016/b978-044450974-1/50018-5
43. Pays, K. (2002). *Double emulsions: how does release occur?* *Journal of Controlled Release*, 79(1-3), 193–205. doi:10.1016/s0168-3659(01)00535-1
44. Garti, N., & Bisperink, C. (1998). *Double emulsions: Progress and applications*. *Current Opinion in Colloid & Interface Science*, 3(6), 657–667. doi:10.1016/s1359-0294(98)80096-4
45. Leister, & Karbstein. (2020). *Evaluating the Stability of Double Emulsions—A Review of the Measurement Techniques for the Systematic Investigation of Instability Mechanisms*. *Colloids and Interfaces*, 4(1), 8. doi:10.3390/colloids4010008
46. Xu, S., Nisisako, T. Polymer Capsules with Tunable Shell Thickness Synthesized via Janus-to-core shell Transition of Biphasic Droplets Produced in a Microfluidic Flow-Focusing Device. *Sci Rep* 10, 4549 (2020). <https://doi.org/10.1038/s41598-020-61641-8>
47. Baret, J.-C. (2012). *Surfactants in droplet-based microfluidics*. *Lab Chip*, 12(3), 422–433. doi:10.1039/c1lc20582j
48. Characteristic Features of Surfactants. (2012). *Surfactants and Interfacial Phenomena*, 1–38. doi:10.1002/9781118228920.ch1
49. Krafft D, López Castellanos S, Lira RB, Dimova R, Ivanov I, Sundmacher K. Compartments for Synthetic Cells: Osmotically Assisted Separation of Oil from Double Emulsions in a Microfluidic Chip. *Chembiochem*. 2019;20(20):2604-2608. doi:10.1002/cbic.201900152

50. Nooranidoost M., Izbassarov D., Muradoglu M. Droplet formation in a flow focusing configuration: Effects of viscoelasticity. *Phys. Fluids*. 2016;28:123102. doi: 10.1063/1.4971841.
51. Nooranidoost M., Haghshenas M., Muradoglu M., Kumar R. Cell encapsulation modes in a flow-focusing microchannel: Effects of shell fluid viscosity. *Microfluid. Nanofluidics*. 2019;23:31. doi: 10.1007/s10404-019-2196-z.
52. DE MENECH, M., GARSTECKI, P., JOUSSE, F., & STONE, H. A. (2008). *Transition from squeezing to dripping in a microfluidic T-shaped junction*. *Journal of Fluid Mechanics*, 595. doi:10.1017/s002211200700910x
53. Takeuchi S., Garstecki P., Weibel D.B., Whitesides G.M. An axisymmetric flow-focusing microfluidic device. *Adv. Mater.* 2005;17:1067–1072. doi: 10.1002/adma.200401738.
54. Gupta A., Kumar R. Effect of geometry on droplet formation in the squeezing regime in a microfluidic T-junction. *Microfluid. Nanofluidics*. 2010;8:799–812. doi: 10.1007/s10404-009-0513-7.
55. Wehking J.D., Gabany M., Chew L., Kumar R. Effects of viscosity, interfacial tension, and flow geometry on droplet formation in a microfluidic T-junction. *Microfluid. Nanofluidics*. 2014;16:441–453. doi: 10.1007/s10404-013-1239-0.
56. Dendukuri, D., & Doyle, P. S. (2009). *The Synthesis and Assembly of Polymeric Microparticles Using Microfluidics*. *Advanced Materials*, 21(41), 4071–4086. doi:10.1002/adma.200803386
57. Alkayyali T., Cameron T., Haltli B., Kerr R., Ahmadi A. Microfluidic and cross-linking methods for encapsulation of living cells and bacteria—A review. *Anal. Chim. Acta*. 2019;1053:1–21. doi: 10.1016/j.aca.2018.12.056.
58. Cramer, C., Fischer, P., & Windhab, E. J. (2004). *Drop formation in a co-flowing ambient fluid*. *Chemical Engineering Science*, 59(15), 3045–3058. doi:10.1016/j.ces.2004.04.006
59. Guerrero, J., Chang, Y., Fragkopoulos, A. A., & Fernandez-Nieves, A. (2019). *Capillary-Based Microfluidics—Coflow, Flow-Focusing, Electro-Coflow, Drops, Jets, and Instabilities*. *Small*, 1904344. doi:10.1002/sml.201904344
60. Saitakis M, Dogniaux S, Goudot C, et al. Different TCR-induced T lymphocyte responses are potentiated by stiffness with variable sensitivity. *Elife*. 2017;6:e23190. Published 2017 Jun 8. doi:10.7554/eLife.23190
61. Harrison, D. L., Fang, Y., & Huang, J. (2019). *T-Cell Mechanobiology: Force Sensation, Potentiation, and Translation*. *Frontiers in Physics*, 7. doi:10.3389/fphy.2019.00045
62. Majedi FS, Hasani-Sadrabadi MM, Thauland TJ, Li S, Bouchard LS, Butte MJ. T-cell activation is modulated by the 3D mechanical microenvironment. *Biomaterials*. 2020;252:120058. doi:10.1016/j.biomaterials.2020.120058
63. <https://geekymedics.com/immune-response/>